EXTENDED PDF FORMAT
SPONSORED BY
IMMUNOLOGY2013™ Travel Grants
from R&D Systems
$1000 travel grants will be awarded to 10 immunology researchers
Apply Now!
www.rndsystems.com



Microbial Exposure During Early Life Has Persistent Effects on Natural Killer T Cell Function

Torsten Olszak *et al.*

Science **336**, 489 (2012);
DOI: 10.1126/science.1219328

This copy is for your personal, non-commercial use only.

If you wish to distribute this article to others, you can order high-quality copies for your colleagues, clients, or customers by clicking here.

Permission to republish or repurpose articles or portions of articles can be obtained by following the guidelines here.

The following resources related to this article are available online at www.sciencemag.org (this information is current as of January 27, 2013):

Updated information and services, including high-resolution figures, can be found in the online version of this article at:
http://www.sciencemag.org/content/336/6080/489.full.html

Supporting Online Material can be found at:
http://www.sciencemag.org/content/suppl/2012/03/21/science.1219328.DC1.html
http://www.sciencemag.org/content/suppl/2012/03/22/science.1219328.DC2.html

A list of selected additional articles on the Science Web sites **related to this article** can be found at:
http://www.sciencemag.org/content/336/6080/489.full.html#related

This article **cites 37 articles**, 12 of which can be accessed free:
http://www.sciencemag.org/content/336/6080/489.full.html#ref-list-1

This article has been **cited by** 12 articles hosted by HighWire Press; see:
http://www.sciencemag.org/content/336/6080/489.full.html#related-urls

This article appears in the following **subject collections:**
Immunology
http://www.sciencemag.org/cgi/collection/immunology

Downloaded from www.sciencemag.org on January 27, 2013

Science (print ISSN 0036-8075; online ISSN 1095-9203) is published weekly, except the last week in December, by the American Association for the Advancement of Science, 1200 New York Avenue NW, Washington, DC 20005. Copyright 2012 by the American Association for the Advancement of Science; all rights reserved. The title *Science* is a registered trademark of AAAS.

from *Pdcd1*$^{-/-}$ mice contained antibodies specific for components of commensal bacteria, which indicated a breach of normal mucosal-systemic compartmentalization (fig. S4, A and C) (*24*). On the basis of the data presented here, we propose that the skewed gut microbial communities that result from the dysregulated selection of IgAs drive the expansion of self-reactive B and T cells. Our studies have implications for how modulation of PD-1 expression promotes tolerance or uncontrolled immune reactions leading to autoimmunity.

References and Notes

1. S. Fagarasan, S. Kawamoto, O. Kanagawa, K. Suzuki, *Annu. Rev. Immunol.* **28**, 243 (2010).
2. J. Jacob, G. Kelsoe, K. Rajewsky, U. Weiss, *Nature* **354**, 389 (1991).
3. M. Muramatsu *et al.*, *Cell* **102**, 553 (2000).
4. N. M. Haynes *et al.*, *J. Immunol.* **179**, 5099 (2007).
5. T. Okazaki, T. Honjo, *Trends Immunol.* **27**, 195 (2006).
6. H. Nishimura, M. Nose, H. Hiai, N. Minato, T. Honjo, *Immunity* **11**, 141 (1999).
7. H. Nishimura *et al.*, *Science* **291**, 319 (2001).
8. T. Okazaki *et al.*, *J. Exp. Med.* **208**, 395 (2011).
9. R. E. Ley *et al.*, *Proc. Natl. Acad. Sci. U.S.A.* **102**, 11070 (2005).
10. L. A. van der Waaij, P. C. Limburg, G. Mesander, D. van der Waaij, *Gut* **38**, 348 (1996).
11. U. Hershberg, M. Uduman, M. J. Shlomchik, S. H. Kleinstein, *Int. Immunol.* **20**, 683 (2008).
12. Materials and methods are available as supplementary materials on *Science* Online.
13. H. E. Mei *et al.*, *Blood* **116**, 5181 (2010).
14. A. Sakaue-Sawano *et al.*, *Cell* **132**, 487 (2008).
15. S. Yuvaraj *et al.*, *J. Immunol.* **183**, 4871 (2009).
16. G. D. Victora *et al.*, *Cell* **143**, 592 (2010).
17. C. D. Allen, T. Okada, H. L. Tang, J. G. Cyster, *Science* **315**, 528 (2007).
18. T. A. Schwickert *et al.*, *J. Exp. Med.* **208**, 1243 (2011).
19. C. G. Vinuesa, S. G. Tangye, B. Moser, C. R. Mackay, *Nat. Rev. Immunol.* **5**, 853 (2005).
20. H. Kwon *et al.*, *Immunity* **31**, 941 (2009).
21. K. L. Good-Jacobson *et al.*, *Nat. Immunol.* **11**, 535 (2010).
22. M. Tsuji *et al.*, *Science* **323**, 1488 (2009).
23. M. Wei *et al.*, *Nat. Immunol.* **12**, 264 (2011).
24. E. Slack *et al.*, *Science* **325**, 617 (2009).

Acknowledgments: We thank T. Honjo, T. Okazaki, T. Okada, I. Taniuchi, O. Kanagawa, N. Minato, and S. Casola for inspiring discussions, suggestions, and critical comments; M. Miyajima and D. Sutherland for critically reading of the manuscript; and Y. Murahashi and T. Kaji for technical assistance. The data reported in this paper are tabulated in the main paper and the supplementary materials. Supported by Grants-in-Aid for Scientific Research in Priority Areas (S.F.) and by RIKEN President's Discretionary Fund (S.F.) and Special Postdoctoral Researchers Program (S.K.).

Supplementary Materials

www.sciencemag.org/cgi/content/full/336/6080/485/DC1
Materials and Methods
Figs. S1 to S4
References (*25*–*34*)

9 December 2011; accepted 16 March 2012
10.1126/science.1217718

Microbial Exposure During Early Life Has Persistent Effects on Natural Killer T Cell Function

Torsten Olszak,[1]* Dingding An,[2]* Sebastian Zeissig,[3] Miguel Pinilla Vera,[4] Julia Richter,[5] Andre Franke,[6] Jonathan N. Glickman,[7] Reiner Siebert,[5] Rebecca M. Baron,[4] Dennis L. Kasper,[2]†‡ Richard S. Blumberg[1]†‡

Exposure to microbes during early childhood is associated with protection from immune-mediated diseases such as inflammatory bowel disease (IBD) and asthma. Here, we show that in germ-free (GF) mice, invariant natural killer T (iNKT) cells accumulate in the colonic lamina propria and lung, resulting in increased morbidity in models of IBD and allergic asthma as compared with that of specific pathogen-free mice. This was associated with increased intestinal and pulmonary expression of the chemokine ligand CXCL16, which was associated with increased mucosal iNKT cells. Colonization of neonatal—but not adult—GF mice with a conventional microbiota protected the animals from mucosal iNKT accumulation and related pathology. These results indicate that age-sensitive contact with commensal microbes is critical for establishing mucosal iNKT cell tolerance to later environmental exposures.

The mammalian host immune system is broadly stimulated with the first exposure to microorganisms during neonatal life (*1*). The inner surfaces of the gastrointestinal tract and lungs are particularly affected because they are predominant sites of microbial contact (*2*). Epidemiologic observations further suggest that the immune effects of early-life microbial exposure are durable and persist into later life because they can be associated with prevention of diseases such as inflammatory bowel disease (IBD) and asthma (*3*–*5*).

Invariant natural killer T (iNKT) cells probably play an important role in the pathogenesis of ulcerative colitis (UC)—a major form of IBD—and in asthma (*6*, *7*). Such cells recognize endogenous and exogenous lipid antigens presented by the nonpolymorphic major histocompatibility complex (MHC) class I–like protein CD1d and secrete abundant amounts of proinflammatory cytokines such as interleukin-4 (IL-4) and IL-13 upon activation (*8*, *9*). We therefore investigated age-dependent regulation of iNKT cells by use of microbes in mouse models of IBD and asthma.

We first examined the appearance of iNKT cells in tissues of 8-week-old germ-free (GF) and specific pathogen-free (SPF) Swiss-Webster (SW) mice. Relative and absolute numbers of iNKT cells were increased in GF mice in colonic lamina propria (LP) (Fig. 1, A to C). These differences in colonic iNKT cell numbers between GF and SPF mice were detectable after weaning and stable for life, suggesting early and persistent effects of the microbiota (Fig. 1D). iNKT cells were not increased in the ileal LP (ileum) of GF mice, and the liver, spleen, and thymus contained even fewer iNKT cells under GF relative to SPF conditions (fig. S1), which is consistent with a recent report (*10*). GF C57BL/6 mice (B6) exhibited similar increases of iNKT cells in the colonic LP as well as the liver, in contrast to GF SW mice (fig. S2). Although increased in number, the iNKT cell expression of several activation and memory markers was unaltered in GF SW, relative to SPF, mice (fig. S3).

To examine the relevance of these findings, we investigated the susceptibility of GF and SPF mice to oxazolone-induced colitis, a model of intestinal inflammation that possesses features of UC and is dependent on IL-13 production by CD1d-restricted iNKT cells (*11*, *12*). Although GF or germ-reduced mice exhibit exacerbated inflammation in an innate mouse model of colitis (*13*, *14*), colitis is typically prevented under GF conditions in models dependent on an adaptive immune response (*15*). Surprisingly, GF mice were more sensitive to oxazolone-induced colitis, as revealed by severe weight loss, pathology, and a high mortality rate in contrast to SPF mice (Fig. 1, E to H). This was not due to overexpression of cell-surface CD1d expression on intestinal epithelial (fig. S4A) and hematopoietic cells (fig. S4B). Consistent with previous studies (*11*), the

[1]Division of Gastroenterology, Hepatology, and Endoscopy, Brigham and Women's Hospital, Harvard Medical School, Boston, MA 02115, USA. [2]Channing Laboratory, Brigham and Women's Hospital and Department of Microbiology and Immunobiology, Harvard Medical School, Boston, MA 02115, USA. [3]Department of Internal Medicine I, University Medical Center Schleswig-Holstein, Kiel 24105, Germany. [4]Division of Pulmonary and Critical Care Medicine, Brigham and Women's Hospital, Harvard Medical School, Boston, MA 02115, USA. [5]Institute of Human Genetics, Christian-Albrechts University Kiel and University Medical Center Schleswig-Holstein, Kiel 24105, Germany. [6]Institute of Clinical Molecular Biology, Christian-Albrechts University, Kiel 24105, Germany. [7]GI Pathology, Caris Diagnostics, Caris Life Sciences, Newton, MA 02464, USA.

*These authors contributed equally to this work.
†These authors contributed equally to this work.
‡To whom correspondence should be addressed. E-mail: rblumberg@partners.org (R.S.B.); dennis_kasper@hms.harvard.edu (D.L.K.)

Downloaded from www.sciencemag.org on January 27, 2013

colitis in GF mice was characterized by a marked increase in production of IL-13 and IL-1β in comparison with SPF mice (Fig. 1I).

To confirm the CD1d-restriction of this colitis in GF mice, we investigated the effects of CD1d blockade. Adult (8- to 9-week-old) GF and SPF mice were treated with a blocking monoclonal antibody (Ab) specific for CD1d (19G11) or an isotype control Ab (*16*). Treatment of GF mice

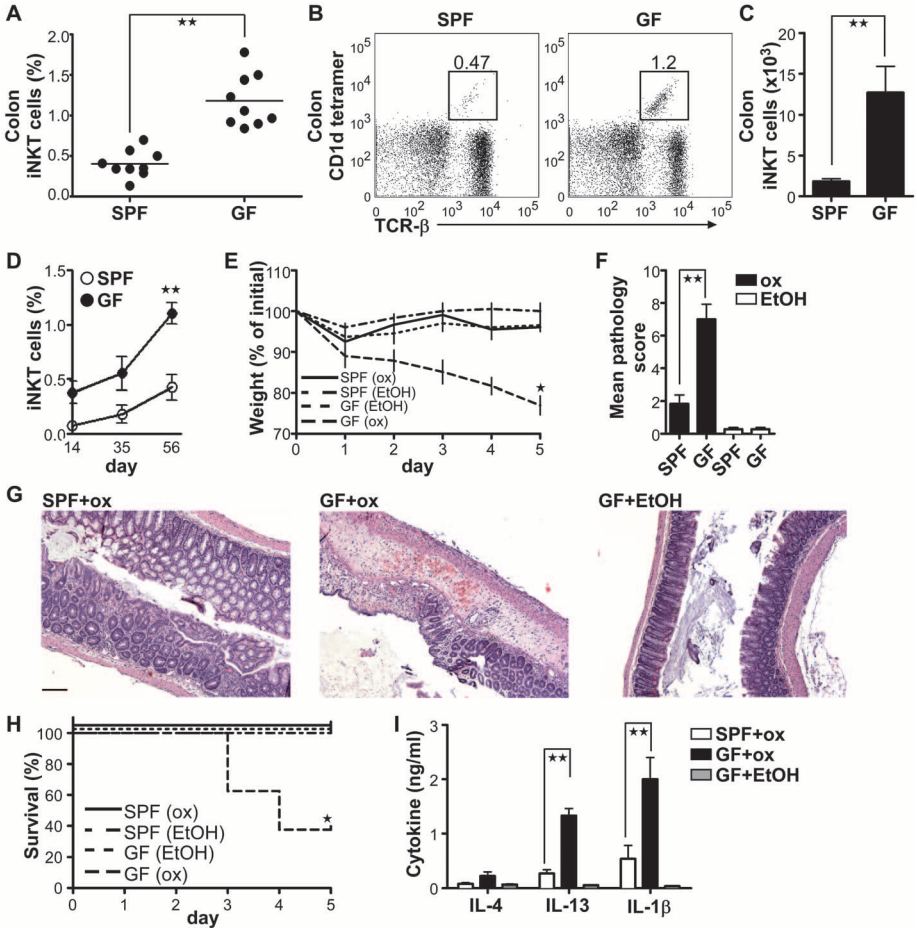


Fig. 1. Intestinal bacteria-dependent accumulation of colonic iNKT cells in GF mice leads to high mortality in oxazolone-induced colitis. (**A** to **C**) The percentage of CD1d tetramer–positive cells (iNKT cells) within the live lymphocytes from the lamina propria (LP) of gender-matched GF and SPF SW mice (7 to 8 weeks old) was analyzed by means of flow cytometry (A). Representative dot-plots are shown in (B), and the absolute number of iNKT cells is shown in (C). Each circle in (A) represents an individual mouse. (**D**) Percentages of colonic iNKT cells of live LP lymphocytes in gender-matched SPF and GF mice were analyzed at different ages by means of flow cytometry ($n = 4$ mice per group). (**E** to **H**) Eight-week-old GF and SPF mice were monitored and scored after rectal challenge with 1% oxazolone (ox) or 50% ethanol for survival and body weight loss for 5 days. On day 5, the colons were collected and dissected for histological analysis ($n = 5$ mice per group). (G) Scale bar, 50 μm. (**I**) The concentration of IL-4, IL-13, and IL-1β in the supernatant of 24 hours–colon organ explant cultures determined by means of enzyme-linked immunosorbent assay (ELISA) on day five ($n = 5$ mice per group). All data were obtained from three independent experiments with similar results. In all panels, error bars represent the SD. $^*P < 0.05$, $^{**}P < 0.01$, unpaired t test and $^*P < 0.05$, log-rank test in (H).

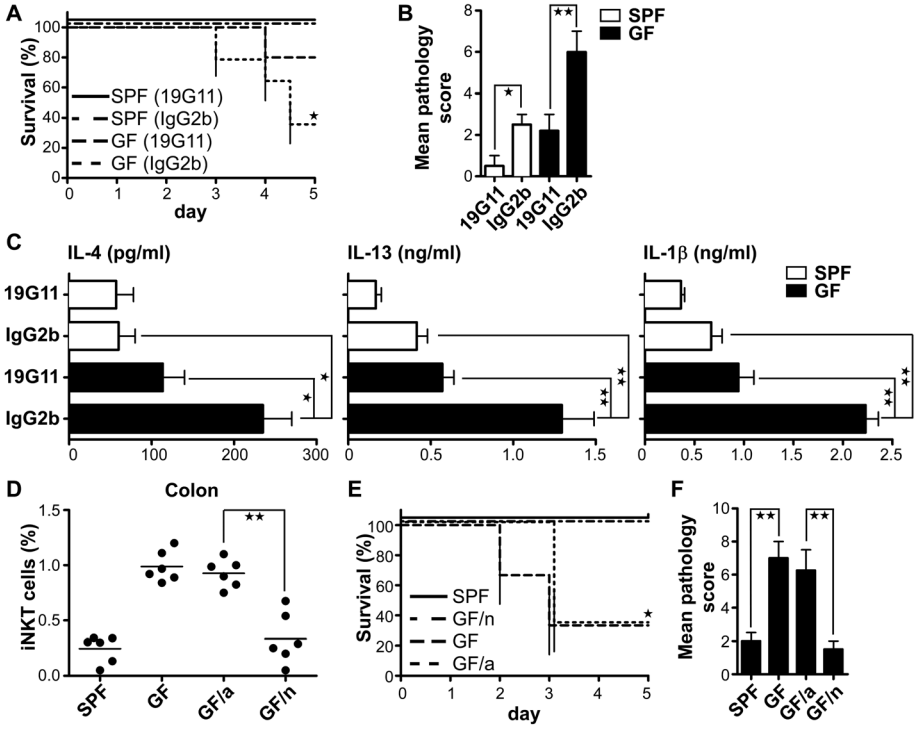


Fig. 2. Microbial colonization during early life prevents the CD1d/iNKT cell-dependent high mortality in oxazolone colitis in GF mice. (**A** to **C**) Eight-week-old GF and SPF mice were treated once with 1 mg of 19G11 or isotype control IgG2b antibody before presensitization and rectal oxazolone challenge. (A) Survival after oxazalone challenge is shown. (B) On day 5, the colons were collected for histological analysis, and (C) the cytokine concentration in the supernatant of 24 hours-colon organ explant cultures was measured with ELISA ($n \geq 4$ mice per group). (**D**) Colonic LP lymphocytes were analyzed for iNKT cells by flow cytometry. (GF/a) mice were GF mice that were exposed to SPF environmental conditions at the age of 5 weeks and maintained for 4 more weeks. (GF/n) mice were pups exposed to SPF conditions on their first day of life and maintained under SPF environmental conditions for 8 to 9 weeks. Each circle represents a mouse. (**E** to **F**) Colonized mice were treated as above with oxazolone ($n = 5$ mice per group). All data were obtained from more than two independent experiments with similar results. Error bars indicate SD. $^*P < 0.05$, $^{**}P < 0.01$, unpaired t test and $^*P < 0.05$, log-rank test in (A) and (E).

Downloaded from www.sciencemag.org on January 27, 2013

with 19G11, but not the isotype control, protected against colitis-induced mortality and associated pathology (Fig. 2, A to C, and fig. S4, C and D). Furthermore, CD1d blockade of GF or SPF mice did not lead to significant functional changes in dendritic cells (*17*) or B cells (*18*) as demonstrated by stable IL-12 or IL-10 production (fig. S4, E and F), respectively.

We next examined whether reestablishing microbiota in adult GF mice would normalize iNKT cell levels in the colon. Quite surprisingly, exposure of adult GF mice to SPF conditions (GF/a) did not restore iNKT cells in the colon to the levels observed in SPF mice or reverse the mortality and severe pathology after oxazolone administration (Fig. 2, D to F). We therefore considered whether the ability to normalize iNKT cell levels and function in the colon was dependent on the

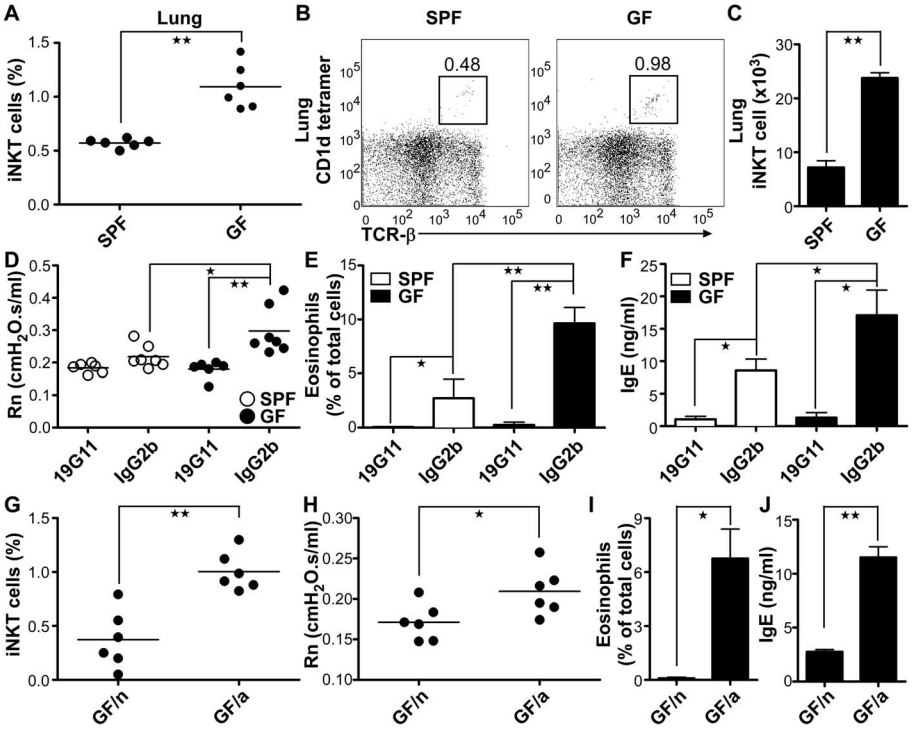


Fig. 3. The increased CD1d/iNKT cell-mediated allergic response sensitivity of GF mice is dependent on age of colonization. (**A** to **C**) Lymphocytes from lungs of 8-week-old mice in each group were analyzed for iNKT cells by means of flow cytometry (A). Representative dot-plot is shown in (B), and the absolute number of iNKT cells is shown in (C) ($n = 6$ mice per group). (**D** to **F**) Age-matched mice from each group were treated once before OVA presensitization with 1 mg of 19G11 or IgG2b isotype control antibody and with 0.5 mg of 19G11 or IgG2b antibody before the first and the third serial OVA exposure. Twenty-four hours after the last challenge with 5% aerosolized OVA, the mice were analyzed for (D) airway resistance (Rn), (E) percentage of eosinophils of total BALF cells, and (F) IgE ($n = 4$ mice per group). (**G**) Lung lymphocytes were analyzed for iNKT cells by means of flow cytometry of age- and gender-matched GF/n and GF/a mice. (**H** to **J**) Mice were presensitized with OVA and analyzed ater the last serial OVA challenge as described above ($n \geq 4$ mice per group). Each circle in (A), (D), (G), and (H) represents an individual mouse. All data were obtained from more than two independent experiments with similar results. Error bars indicate the SD. $^*P \leq 0.05$, $^{**}P < 0.01$, unpaired *t* test.

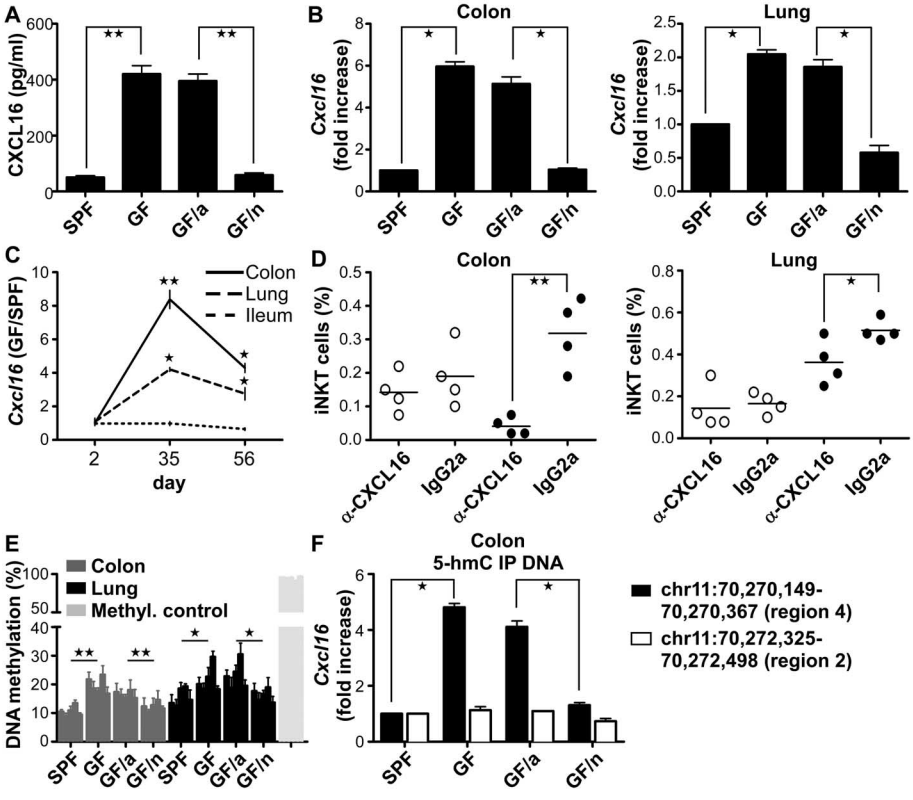


Fig. 4. Microbiota affects tissue specific iNKT cell accumulation by genetic modifications of *Cxcl16*. (**A**) The CXCL16 concentration in the serum of each group was measured with ELISA in SPF, GF, GF/a, and GF/n as described above ($n = 4$ mice per group). (**B**) Colon and lung tissue samples were harvested from age-matched mice from each group and analyzed for *Cxl16* expression ($n = 4$ mice per group). (**C**) Colon, ileum, and lung tissue samples were analyzed from age-matched SPF and GF mice at different time points for *Cxcl16* expression ($n = 5$ mice per group). (**D**) SPF (open circles) and GF (closed circles) newborn mice were treated three times a week intraperitoneal with 25 μg of a neutralizing CXCL16 antibody (αCXCL16) or its isotype control IgG2a antibody and analyzed at the age of 2 weeks for iNKT cell percentages by means of flow cytometry. Each circle represents a mouse. (**E**) Analysis of DNA methylation of five CpG sites of *Cxcl16* by bisulfite pyrosequencing. For each group, the mean of DNA methylation of 5 CpG sites is shown as a percentage according to the methylated control (Methyl. control) ($n \geq 3$ mice per group). (**F**) *Cxcl16* qPCR analysis of colonic DNA after performing a 5-hydroxymethylated DNA immunoprecipitation (5-hmC IP DNA) ($n \geq 3$ mice per group). All data were obtained from at least two independent experiments with similar results. Error bars indicate the SD. $^*P \leq 0.05$, $^{**}P < 0.01$, unpaired *t* test.

Downloaded from www.sciencemag.org on January 27, 2013

age at which microbial contact occurred. Indeed, when we colonized pregnant GF female mice just before delivery and therefore exposed neonatal GF mice to SPF conditions on their first day of life (GF/n), we observed a complete normalization of iNKT cell levels that persisted even two months after colonization (Fig. 2D). Consistent with this, GF/n exhibited reduced susceptibility to oxazolone-induced colitis (relative to that of GF mice) two months after colonization, with a degree of severity identical to that observed in SPF animals, as shown by an analysis of mortality, weight loss, pathology, and cytokine production (Fig. 2, E and F, and fig. S5).

To verify that the early life events associated with the absence of normal microbial colonization on iNKT cell homeostasis were CD1d-dependent, we treated GF mice with 19G11 Ab for their first 6 weeks of life. 19G11, but not control Ab, treatment blocked accumulation of iNKT cells in all tissues examined and susceptibility to oxazolone-induced colitis in later life (fig. S6). Similar to GF mice, SPF mice (B6) born under germ-reduced conditions exhibited an increase in colonic iNKT cells and excessive oxazolone-induced colitis at 4 weeks of life (fig. S7). As predicted (*11*), $Cd1d^{-/-}$ and $J\alpha18^{-/-}$ mice, both of which lack iNKT cells, were not susceptible to oxazolone-induced colitis either under SPF or germ-reduced conditions (fig. S7).

Animal models of asthma demonstrate an important role for iNKT cells (*19*, *20*), although the contribution to human disease remains controversial (*21*). We found that the lungs of GF SW and B6 mice contained significantly higher relative and absolute numbers of iNKT cells in comparison with that of the lungs of the respective SPF mice (Fig. 3, A to C, and fig. S8). Because commensal microbes may affect the induction of experimental asthma (*22*), we tested an ovalbumin (OVA)–driven allergic-asthma mouse model in GF mice. We observed that similar to the colon, GF mice developed an allergic airway response to OVA significantly greater than that observed in SPF mice, as demonstrated by increases in airway resistance, total bronchial alveolar lavage fluid (BALF) cell numbers, BALF eosinophilia, serum immunoglobulin E (IgE) levels, proinflammatory cytokine production in the BALF, and lung tissue eosinophil infiltration (Fig. 3, D to F, and fig. S9). The asthma in GF mice was CD1d- and antigen-dependent because elimination of the asthmatic response was only observed with 19G11, but not control, Ab treatment (Fig. 3, D to F, and fig. S9) of OVA-sensitized mice but not mice exposed to phosphate-buffered saline (PBS), which did not induce allergic asthma (fig. S10).

We therefore next investigated whether early-life exposure to a conventional microbiota also protects animals from CD1d-restricted inflammation in the lungs. As observed in the intestinal mucosa, neonatal (GF/n)—but not adult-life (GF/a)—exposure of GF mice to a conventional microbiota abrogated the increased accumulation of iNKT cells in the lungs and protected adult mice in the allergic asthma model from the pathology (Fig. 3, G to I, and fig. S11).

The chemokine receptor CXCR6 on iNKT cells (*23*) and its ligand CXCL16, which is expressed at high levels by human epithelial cells (*24*) and increased in inflammation (*25*), plays an important role in iNKT cell homeostasis. Therefore, we examined the serum of GF and GF/a mice for the presence of CXCL16 and observed significantly higher levels than that observed in SPF and GF/n mice (Fig. 4A). This was due to significant increases of *Cxcl16* mRNA expression levels in the colon and lung—but not ileum, liver, and thymus—of GF and GF/a relative to SPF and GF/n mice (Fig. 4B and fig. S12A), and mainly immunolocalized to the epithelium (fig. S12B). Although *Cxcl16* mRNA levels in the colon, ileum, and lung were similar immediately after birth in the GF and SPF animals at the beginning of colonization, they increased significantly and specifically only in the colon and lungs of the GF mice during later life (Fig. 4C). These results suggest that microbial exposure provides signals that determine *Cxcl16* gene expression in specific tissues. GF and SPF mice, however, exhibited similar levels of *Cxcr6* mRNA expression in tissues and CXCR6 expression on the cell surface of iNKT cells (fig. S12, C and D).

CXCL16 was responsible for the accumulation of iNKT cells because treatment of newborn SPF and GF mice with a CXCL16-neutralizing Ab caused a decrease in iNKT cells in the colon and lung (Fig. 4D) but had no effect on iNKT cell levels in the ileum or thymus (fig. S13A). However, it was associated with an increased accumulation of iNKT cells in the liver (fig. S13A), suggesting CXCL16 blockade caused a redirection of iNKT cells to this organ. Consequently, Ab-to-CXCL16– but not isotype-treated GF mice were protected from oxazolone colitis–induced mortality and pathology (fig. S13, B to D).

We next examined the epigenetic content of the *Cxcl16* gene of GF and SPF mice. A region 5′ of the *Cxcl16* gene of SW mice that contains five potential CpG sites was determined by means of bisulfite pyrosequencing to be hypermethylated in the colon and lungs (Fig. 4E)—but not in other tissues such as the spleen and liver (fig. S14)—under GF conditions as compared with SPF conditions. Colonization of neonatal —but not adult—GF mice with a conventional microbiota decreased the hypermethylation of the *Cxcl16* gene to SPF levels (Fig. 4E). Gene activation due to hypermethylation may occur as a consequence of specific types of environmental exposure (*26*). To confirm this, we treated SPF neonates on their first day of life by oral gavage with high doses of folinic acid as previously described (*27*) so as to force *Cxcl16* methylation. Compared with PBS-treated control mice, folinic acid administration resulted in elevated methylation of the *Cxcl16* gene in the colon, ileum, and lung; at least a three- to fourfold increase of *Cxcl16* mRNA expression in the same tissues; increased CXCL16 serum levels; and accumulation of iNKT cells in these tissues as observed in GF mice (fig. S15). Alternatively, we investigated whether elimination of *Cxcl16* methylation in GF mice would reverse the elevation of CXCL16 expression by treating GF newborn littermates with the DNA methyltransferase inhibitor 5-Azacytidine (5-Aza). When examined at 2 weeks of life, 5-Aza treatment inhibited methylation and mRNA expression of *Cxcl16* in the colon, ileum, and lung (fig. S16, A and B), diminished the levels of CXCL16 in the serum, and reduced iNKT cells in these tissues (fig. S16, C and D). 5-Aza treatment had no effect on other cell populations such as $CD45^{+}CD11c^{+}$ double positive cells (fig. S17).

Epigenetic marks provided by 5-hydroxymethylcytosine (5-hmC) incorporation into DNA have been suggested to be different from those provided by 5-methylcytosine (5-mC) and a distinct signature for elevated levels of transcription (*28*). We therefore performed DNA immunoprecipitation with a monoclonal 5-hmC Ab followed by quantitative polymerase chain reaction (PCR) analysis for *Cxcl16* in seven different regions of *Cxcl16* in DNA samples obtained from the colons of SPF, GF, GF/a, and GF/n mice. We observed that *Cxcl16* was highly increased in three out of the seven investigated regions (with region 4 as a representative) within the 5-hmC–modified DNA of GF and GF/a mice but not in the DNA acquired from SPF and GF/n mice (Fig. 4F). No differences were observed in the other four regions (with region 2 as a representative) and in the DNA samples obtained from the ileum demonstrating the colonic specificity for 5-hmC modification of *Cxcl16* (fig. S18). A map summarizing this information is provided in fig. S19.

Our studies indicate that CXCL16 is an age- and organ-dependent microbially regulated factor that modulates the quantities and function of iNKT cells in the colon and lungs and, consequently, susceptibility to tissue inflammation. The exact mechanism by which the microbiota regulates CXCL16 expression and thus iNKT cell accumulation in these organs is unknown, although it is independent of the Toll-like receptor adapter protein MyD88 (fig. S20). These observations are in accordance with previous epidemiological studies collectively known as the "hygiene hypothesis," which proposes that early-life exposure to specific microbe-enriched environments decreases susceptibility to diseases such as IBD and asthma (*3*, *5*, *29*, *30*), whereas its absence, as in antibiotic treatment during childhood, may have the opposite effect (*31*, *32*). Our results suggest that CD1d-restricted iNKT cell pathways and their relationship to microbes play a central role in these aforementioned processes. Early-life microbial exposure elicits long-lasting effects on iNKT cells, and in their absence, later-life exposure to factors that stimulate these cells may induce an autoinflammatory response. These findings are predicted to extrapolate to humans, given the extensive similarities between the mouse and human CD1d and iNKT cell systems (*33*).

Downloaded from www.sciencemag.org on January 27, 2013

References and Notes

1. D. Kelly, T. King, R. Aminov, *Mutat. Res.* **622**, 58 (2007).
2. H. Renz *et al.*, *Nat. Rev. Immunol.* **12**, 9 (2012).
3. M. J. Ege *et al.*; GABRIELA Transregio 22 Study Group, *N. Engl. J. Med.* **364**, 701 (2011).
4. P. López-Serrano *et al.*, *Scand. J. Gastroenterol.* **45**, 1464 (2010).
5. E. von Mutius, *Immunobiology* **212**, 433 (2007).
6. O. Akbari *et al.*, *Nat. Med.* **9**, 582 (2003).
7. I. J. Fuss *et al.*, *J. Clin. Invest.* **113**, 1490 (2004).
8. N. R. Cohen, S. Garg, M. B. Brenner, *Adv. Immunol.* **102**, 1 (2009).
9. M. Kronenberg, *Annu. Rev. Immunol.* **26**, 877 (2005).
10. B. Wei *et al.*, *J. Immunol.* **184**, 1218 (2010).
11. F. Heller, I. J. Fuss, E. E. Nieuwenhuis, R. S. Blumberg, W. Strober, *Immunity* **17**, 629 (2002).
12. G. Schiechl *et al.*, *J. Clin. Invest.* **121**, 1692 (2011).
13. K. M. Maslowski *et al.*, *Nature* **461**, 1282 (2009).
14. S. Rakoff-Nahoum, J. Paglino, F. Eslami-Varzaneh, S. Edberg, R. Medzhitov, *Cell* **118**, 229 (2004).
15. W. Strober, I. J. Fuss, R. S. Blumberg, *Annu. Rev. Immunol.* **20**, 495 (2002).
16. J. H. Roark *et al.*, *J. Immunol.* **160**, 3121 (1998).
17. S. C. Yue, A. Shaulov, R. Wang, S. P. Balk, M. A. Exley, *Proc. Natl. Acad. Sci. U.S.A.* **102**, 11811 (2005).
18. A. Mizoguchi, A. K. Bhan, *J. Immunol.* **176**, 705 (2006).
19. E. H. Meyer, R. H. DeKruyff, D. T. Umetsu, *Annu. Rev. Med.* **59**, 281 (2008).
20. G. Wingender *et al.*, *J. Exp. Med.* **208**, 1151 (2011).
21. C. Iwamura, T. Nakayama, *Curr. Opin. Immunol.* **22**, 807 (2010).
22. T. Herbst *et al.*, *Am. J. Respir. Crit. Care Med.* **184**, 198 (2011).
23. E. Germanov *et al.*, *J. Immunol.* **181**, 81 (2008).
24. C. Day, R. Patel, C. Guillen, A. J. Wardlaw, *Exp. Lung Res.* **35**, 272 (2009).
25. J. Diegelmann *et al.*, *Inflamm. Bowel Dis.* **16**, 1871 (2010).
26. V. Rishi *et al.*, *Proc. Natl. Acad. Sci. U.S.A.* **107**, 20311 (2010).
27. M. Pufulete *et al.*, *Gut* **54**, 648 (2005).
28. C. X. Song *et al.*, *Nat. Biotechnol.* **29**, 68 (2011).
29. A. S. Neish, *Gastroenterology* **136**, 65 (2009).
30. D. P. Strachan, *BMJ* **299**, 1259 (1989).
31. S. Y. Shaw *et al.*, *Am. J. Gastro.* **105**, 2687 (2010).
32. E. Goksör *et al.*, *Acta Paediatr.* **100**, 1561 (2011).
33. B. A. Sullivan, M. Kronenberg, *Curr. Top. Microbiol. Immunol.* **314**, 165 (2007).

Acknowledgments: We thank E. Troy and S. Edwards for handling of the GF mice, J. Cusick for technical assistance, E. Nieuwenhuis and K. Schneeberger for assistance with epigenetics studies, A. Bellacosa and K. Baker for helpful discussions and manuscript preparation, and the KinderKrebsInitiative Buchholz/Holm-Seppensen for providing pyrosequencing infrastructure. The work was supported by NIH grants DK44319, DK51362, DK53056, and DK88199 (R.S.B.) and AI090102 (D.L.K.); Crohn's Colitis Foundation of America Senior Research Award (D.L.K.) and Crohn's and Colitis Foundation of America Postdoctoral Fellowship Award (D.A. and S.Z.); the Harvard Digestive Diseases Center (DK034854); the Medizinausschuss Schleswig-Holstein, German Ministry of Education Research through the National Genome Research Network (A.F.); The Medical Faculty, Kiel (R.S.) and the Deutsche Forschungsgemeinschaft (DFG) (OL 324/1-1, SZ 814/1-1, 814/4-1); as well as DFG Excellence Cluster "Inflammation at Interfaces" (A.F. and S.Z.). The data reported in this manuscript are tabulated in the main paper and in the supplementary materials.

Supplementary Materials

www.sciencemag.org/cgi/content/full/science.1219328/DC1
Materials and Methods
Figs. S1 to S20
Tables S1 and S2
References (*34*–*37*)

18 January 2012; accepted 6 March 2012
Published online 22 March 2012;
10.1126/science.1219328

Analytic Thinking Promotes Religious Disbelief

Will M. Gervais* and Ara Norenzayan*

Scientific interest in the cognitive underpinnings of religious belief has grown in recent years. However, to date, little experimental research has focused on the cognitive processes that may promote religious disbelief. The present studies apply a dual-process model of cognitive processing to this problem, testing the hypothesis that analytic processing promotes religious disbelief. Individual differences in the tendency to analytically override initially flawed intuitions in reasoning were associated with increased religious disbelief. Four additional experiments provided evidence of causation, as subtle manipulations known to trigger analytic processing also encouraged religious disbelief. Combined, these studies indicate that analytic processing is one factor (presumably among several) that promotes religious disbelief. Although these findings do not speak directly to conversations about the inherent rationality, value, or truth of religious beliefs, they illuminate one cognitive factor that may influence such discussions.

Although most people fervently believe in God or gods, there are nonetheless hundreds of millions of nonbelievers worldwide (*1*), and belief and disbelief fluctuate across situations and over time (*2*). Religious belief and disbelief are likely complex, multidetermined, psychologically and culturally shaped phenomena, yet to date little experimental research has explored the specific cognitive underpinnings of religious disbelief (*3*, *4*). Here we begin to address this important gap in the literature by applying a dual-process cognitive framework, which predicts that analytic thinking strategies might be one potent source of religious disbelief.

According to dual-process theories of human thinking (*5*, *6*), there are two distinct but interacting systems for information processing. One (System 1) relies upon frugal heuristics yielding intuitive responses, while the other (System 2) relies upon deliberative analytic processing. Although both systems can at times run in parallel (*7*), System 2 often overrides the input of system 1 when analytic tendencies are activated and cognitive resources are available. Dual-process theories have been successfully applied to diverse domains and phenomena across a wide range of fields (*5*, *6*, *8*, *9*).

Available evidence and theory suggest that a converging suite of intuitive cognitive processes facilitate and support belief in supernatural agents, which is a central aspect of religious beliefs worldwide (*10*–*13*). These processes include intuitions about teleology (*14*), mind-body dualism (*13*), psychological immortality (*15*), and mind perception (*16*, *17*). Religious belief therefore bears many hallmarks of System 1 processing.

If religious belief emerges through a converging set of intuitive processes, and analytic processing can inhibit or override intuitive processing, then analytic thinking may undermine intuitive support for religious belief. Thus, a dual-process account predicts that analytic thinking may be one source of religious disbelief. Recent evidence is consistent with this hypothesis (*4*), finding that individual differences in reliance on intuitive thinking predict greater belief in God, even after controlling for relevant socio-demographic variables. However, evidence for causality remains rare (*4*). Here we report five studies that present empirical tests of this hypothesis.

We adopted three complementary strategies to test for robustness and generality. First, study 1 tested whether individual differences in the tendency to engage analytic thinking are associated with reduced religious belief. Second, studies 2 to 5 established causation by testing whether various experimental manipulations of analytic processing, induced subtly and implicitly, encourage religious disbelief. These manipulations of analytic processing included visual priming, implicit priming, and cognitive disfluency (*18*, *19*). Third, across studies, we assessed religious belief using diverse measures that focused primarily on belief in and commitment to religiously endorsed supernatural agents. Samples consisted of participants from diverse cultural and religious backgrounds (*20*).

Study 1 was a correlational study with Canadian undergraduates (N = 179). We correlated performance on an analytic thinking task with three related, but distinct, measures of religious belief. The analytic thinking task (*6*) contains three problems that require participants to analytically override an initial intuition. This task was designed to specifically measure analytic processing because an intuitive reading of each problem invites a quick and easy, yet incorrect, response that must be analytically overridden (Table 1). Furthermore, experimental manipulations known to induce analytic processing

University of British Columbia, Vancouver, BC V6T1Z4, Canada.

*To whom correspondence should be addressed. E-mail: will@psych.ubc.ca (W.M.G.); ara@psych.ubc.ca (A.N.)

Downloaded from www.sciencemag.org on January 27, 2013

Correction: 5 April 2012



www.sciencemag.org/cgi/content/full/science.1219328/DC1

Supplementary Material for

Microbial Exposure During Early Life Has Persistent Effects on Natural Killer T Cell Function

Torsten Olszak, Dingding An, Sebastian Zeissig, Miguel Pinilla Vera, Julia Richter, Andre Franke, Jonathan N. Glickman, Reiner Siebert, Rebecca M. Baron, Dennis L. Kasper,* Richard S. Blumberg*

*To whom correspondence should be addressed. E-mail: rblumberg@partners.org (R.S.B.); dennis_kasper@hms.harvard.edu (D.L.K.)

Published 22 March 2012 on *Science* Express
DOI: 10.1126/science.1219328

This PDF file includes:

Materials and Methods

Figs. S1 to S20

Tables S1 to S2

References (*34–37*)

Correction: The authors have corrected a range of typographical errors and minor mislabelings throughout the file.

Materials and Methods

Mice

Swiss Webster (SW) mice kept under SPF or GF conditions were purchased from Taconic USA. GF mice were bred and maintained in vinyl isolators within the animal facility of Harvard University, Boston USA. GF mice on a B6 background were generated and maintained under GF conditions at Taconic USA. *CD1d*$^{-/-}$ and *Jα18*$^{-/-}$ mice were kindly provided by Dr. Mark Exley (Beth Israel Deaconess Medical Center) and were backcrossed onto a C57BL/6 background. C57BL/6 mice were purchased from The Jackson Laboratory and *Myd88*$^{-/-}$ mice were a gift from Shizou Akira (Osaka University, Japan). For the colonization experiments GF/adult (GF/a) mice were GF mice that were exposed to SPF environmental conditions at the age of 5 weeks and maintained for 4 more weeks. GF/neonate (GF/n) mice were pups exposed to SPF conditions on their first day of life and kept under SPF environmental conditions for eight to nine weeks. For some experiments SW SPF newborn littermates were orally gavaged with either 1 mg/ml folinic acid (FA) (Sigma) or PBS 5 times a week for 2 weeks or SW GF newborn littermates received by intraperitoneal (i.p.) injection 2.5 µg per g 5-Azacytidine (Sigma) or PBS on day 1 and day 8 of their lives. All procedures were approved by the Harvard Medical Area Standing Committee on Animals.

Isolation of lymphocytes and flow cytometry

To isolate LP lymphocytes, ileum and large intestines were collected, fat tissue removed, flushed with PBS in order to remove fecal content, inverted and shaken in PBS containing 3% FBS, 5% DTT and 0.5M EDTA for 30 min at 37°C. After removing epithelial cells the intestines were washed in PBS by inverting ten times in a 15 ml Falcon tube, cut into small pieces and incubated with RPMI 1640 containing 5% FBS, 1.5 mg/ml collagenase type II and 0.5 mg/ml dispase (all GIBCO) for 1 h at 37°C under constant horizontal shaking (500 rpm). The digested tissues were filtered through a 40 µm strainer and washed three times in staining buffer containing PBS and 2% FBS and used as LP lymphocytes in flow cytometry. Isolation of lung lymphocytes was performed according to the protocol of Sauer with minor modifications (34). Briefly, the lungs were collected, washed in PBS, cut into small pieces and incubated in a 15 ml Falcon tube with PBS containing 1.3 mg/ml collagenase type II (GIBCO) and 150 µg/ml DNase I (Roche) for 1 h at 37°C under constant horizontal shaking (500 rpm). The digested tissues were filtered through a 40 µm strainer, centrifuged for 5 min at 1500 rpm and incubated in ACK lysis buffer for 5 min at RT. After three washes in staining buffer the cells were used as lung lymphocytes in flow cytometry. Liver lymphocytes were prepared according to the methods of Matsuda with minor modification (35). In brief, after perfusion with 10 ml PBS via portal vein, mouse liver fragments were pressed through 70 µm cell strainer. Total liver cells were then resuspended in a 40% isotonic Percoll solution (Amersham Pharmacia Biotech) underlaid with a 60% isotonic Percoll solution. After centrifugation for 25 minutes at 1500 rpm, mononuclear cells were isolated at the 40/60% interface and washed three times in staining buffer before the cells were used in flow cytometry. To isolate splenic and thymic lymphocytes, the tissues were harvested, filtered through a 40 µm strainer, centrifuged for 5 min at 1500 rpm and incubated in ACK lysis buffer for 5 min at RT. After three washes in staining buffer the cells were used as splenic and thymic lymphocytes in flow cytometry.

The following antibodies were used: PE-labeled PBS57-loaded or unloaded CD1d tetramer (NIH Tetramer Core Facility, Atlanta, GA), APC-Cy7-labeled TCR-β (eBioscience), PE-Cy7-labeled CD62L and IgG2a isotype control (eBioscience), PerCp-labeled CD69 and IgG isotype control (eBioscience), APC-labeled CD45RB and IgG2a isotype control (eBioscience), FITC-labeled-CD1d and isotype control IgG2b (BD), PE- or PerCp-labeled-CD45 (eBioscience), APC-Cy7-labeled-B220 (eBioscience), PE-labeled-CD11b (BD), FITC- or PE-Cy7-labeled CD11c (BD), FITC-labeled CD3 (BD), APC-labeled-CXCR6 and IgG2b isotype control (R&D), APC-labeled-Integrin α4β7 (Biolegend) and Pacific blue-labeled DAPI (Biolegend) were used. Flow cytometry was performed using MACS Quant (Miltenyi Biotec) and data were analyzed with FlowJo software (TreeStar Inc.).

Experimental oxazolone colitis model

Mice were pre-sensitized by epicutaneous application of 3% oxazolone (4-ethoxymethylene-2-phenyl-2-

oxazolin-5-one; Sigma-Aldrich) in 100% ethanol in a volume of 200 µl. Five days after pre-sensitization mice were re-challenged intra-rectally with 150 µl 1% oxazolone in 50% ethanol under anesthesia with 2,2,2-Tribromoethanol (Sigma-Aldrich) using a 3.5 F catheter. For several experiments the mice were treated i.p. with the 19G11 or IgG2b isotype control antibody (BioXcell) and with the CXCL16 monoclonal antibody or its isotype control IgG2a (R&D). Some pregnant females were treated 24 to 48 hours before delivery with sulfatrim (Fisher Scientific) (48 mg/ml in the drinking water) and both the parents and the offspring were kept under sulfatrim for two more weeks. Body weight, rectal bleeding, and stool consistency were analyzed on a daily basis. Tissues obtained at the indicated time points were embedded in paraffin, stained with haematoxylin/eosin (H&E) and examined for evidence of colitis by using five established criteria for colitis activity in a blinded fashion by a pathologist (JG): hypervascularization, presence of mononuclear cells, epithelial hyperplasia, epithelial injury, and presence of granulocytes.

Colon organ culture

Standardized segments (1 cm x 1 cm) of all three parts of the colon were washed in cold PBS supplemented with penicillin and streptomycin (P/S) (GIBCO) and cultured in 24-well flat-bottom-culture plates (Falcon) in serum-free RPMI 1640 media (GIBCO) supplemented with P/S for 24 h at 37°C. Supernatants were analyzed for the cytokines IL-4, IL-10, IL-12, IL-13 and IL-1β by ELISA (all BD).

Experimental allergen-induced airway inflammation

Mice were sensitized using ovalbumin (OVA) (Sigma-Aldrich) at a concentration of 10 µg/mouse in a volume of 200 µl Imject Alum (Thermo Scientific) i.p. on days 0 and 12. Between days 18 and 23 all mice were challenged daily with 5% aerosolized OVA or PBS via the airways for 20 min. The mice were euthanized by exsanguination under terminal anesthesia after completion of the experiments described below.

Pulmonary function tests

For measurement of *in vivo* airway responsiveness the anaesthetized mice were tracheotomized and connected to a small animal ventilator (flexiVent, SCIREQ, Inc.). Airways resistance (Rn), tissue resistance (G) and tissue elastance (H) were measured by fitting the constant phase model to input impedance as described previously (36).

Bronchoalveolar lavage fluid (BALF)

The airways of the mice were lavaged three times with 1 ml PBS via a tracheal cannula. The BALF was centrifuged and the supernatant was removed and analyzed for IL-4, IL-10, IL-12, IL-13 and IL-17 cytokines and IgE by ELISA (all BD ELISA-kits). The cells were recovered and stained after a cytospin with the Hema 3 Staining Kit (Fisher) for cell differentiation as described previously (36).

Bisulfite–pyrosequencing

Genomic DNA (gDNA) from various tissues was prepared using the DNA Mini Kit (Qiagen). Pyrosequencing was performed as described previously and blinded for the sample characteristics (37). Briefly, gDNA was bisulfite converted using the EpiTect Bisulfite Conversion Kit (Qiagen). *Cxcl16* PCR amplification was performed using the PyroMark PCR Kit (Qiagen) according to standard protocol (primer sequences, PCR conditions and analyzed region are shown in Table S1). Amplification was verified by agarose gel electrophoresis. Pyrosequencing was performed using the Pyrosequencer ID and the DNA methylation analysis software Pyro Q-CpG 1.0.9 (Biotage), which was also used to evaluate the ratio T:C (mC:C) at the CpG sites analyzed. The assay was optimized and validated using commercially available completely methylated DNA (ZymoResearch). For each group the mean of the 5 CpG sites of the amount of DNA methylation in percentage according to the methylated control was calculated and statistical significance was determined by the unpaired *t*-test.

Hydroxymethylated DNA immunoprecipitation

5-hydroxymethylated (5-hmC) DNA immunoprecipitation was performed using the hMeDIP kit according to the manufacturer's instructions (Diagenode). Briefly, DNA samples were sheared to an average length of 300-500 bp by exposing the DNA to the energy of adaptive focused acoustic using a Covaris S2 (Covaris) according to the protocol of the manufacturer. After an incubation with magnetic beads coated with the 5-hmC monoclonal antibody or its isotype control IgG, the antibody was magnetically captured and after several wash steps the immunoprecipitated DNA was isolated by using the iPure kit (Diagenode) according to the manufacturer's protocol before qPCR analysis was performed (primer sequences, PCR conditions and analyzed regions are shown in Table S2).

Real-time RT-PCR

RNA samples were prepared using an RNeasy Mini Kit and complementary DNAs were synthesized using the Omniscript RT Kit (all Qiagen). Real-time RT-PCR was performed using a SYBR Green I Master Mix (Roche) and a CFX96 Real-Time System (Bio-Rad). Values were normalized to the expression of β-*Actin* for each sample. The following primer sets were initially tested to confirm comparable efficiencies and used: *Cxcr6*, 5'-TCTTTGGACTGCTAGGAAACTCC-3' and 5'- AGAGTACAGACAAACACCAGGT-3' (NCBI Reference Sequence: NM_030712.4); *Cxcl16*, 5'-CAGATACCGCAGGGTACTTTG-3' and 5'-CTGCAACTGGAACCTGATAAAGA-3' (NCBI Reference Sequence: NM_023158.6); *Ccl25*, 5'-CCAAGGTGCCTTTGAAGACT-3' and 5'-TCCTCCAGCTGGTGGTTACT-3' (NCBI Reference Sequence: NM_009138.3); β-*Actin*, 5'- GATGCTCCCCGGGCTGTATT-3' and 5'- GGGGTACTTCAGGGTCAGGA-3' (NCBI Reference Sequence: NM_007393.3). The NCBI Reference Sequence NC_000077.5 was used for designing the *Cxcl16* gDNA primers and the NCBI Reference Sequence NC_000071.5 was used for the *ACTB* gDNA primers.

Immunohistochemistry

Paraffin embedded tissue sections were deparaffinised and the endoperoxidase and serum blocking steps were then performed before the sections were incubated with the polyclonal goat anti-CXCL16 antibody (1:50) (R&D) or its isotype control IgG2a (1:50) (Abcam) for 18 h at 4°C. After a wash in PBS (5 min), a biotinylated secondary donkey anti-goat antibody (1:100) (Abcam) was applied (30 min) and the sections were washed in PBS (5 min). A solution of streptavidin-conjugated horseradish peroxidase (HRP) was applied to the sections (30 min), prior to a final wash in PBS. Finally, a diaminobenzidine-HRP (DAB-HRP) reaction was performed until such time as immunolocalization was apparent. After counterstaining with hematoxylin the sections were mounted in Permount (Fisher Scientific). All images were taken by a digital camera on a Nikon Eclipse Ti microscope (Nikon Inc., USA).

Statistical analysis

Statistical significance was determined by the unpaired *t*-test. Comparisons of mortality were made by analyzing Kaplan–Meier survival curves, and the log-rank test was used to assess for differences in survival. All *P* values were two-tailed, and statistical significance was accepted at $P < 0.05$.

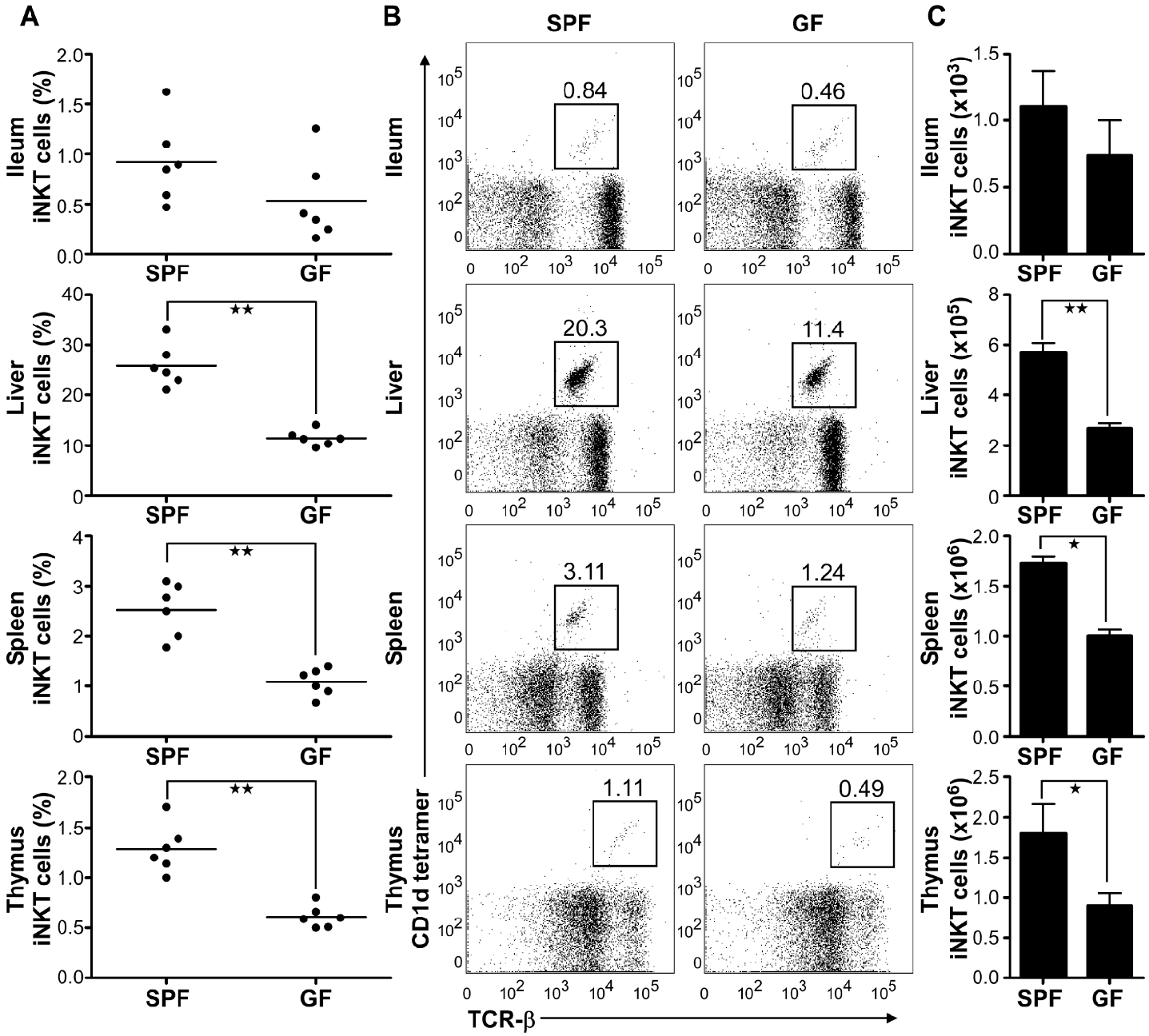


Fig. S1. iNKT cells are increased in ileum, liver, spleen and thymus in Swiss Webster (SW) SPF mice. **(A)** Percentages for CD1d tetramer and TCR-β double positive cells (iNKT) of live lymphocytes from ileum, liver, spleen and thymus of specific-pathogen-free (SPF) and germ-free (GF) mice were analyzed by flow cytometry. Representative dot-plots are shown in **(B)** and total numbers for iNKT cells are shown in **(C)** (n ≥ 5 mice per group). All data were obtained from more than two independent experiments with similar results. Each circle represents a mouse, and error bars indicate SD. *$P \leq 0.05$, **$P < 0.01$, unpaired *t* test.

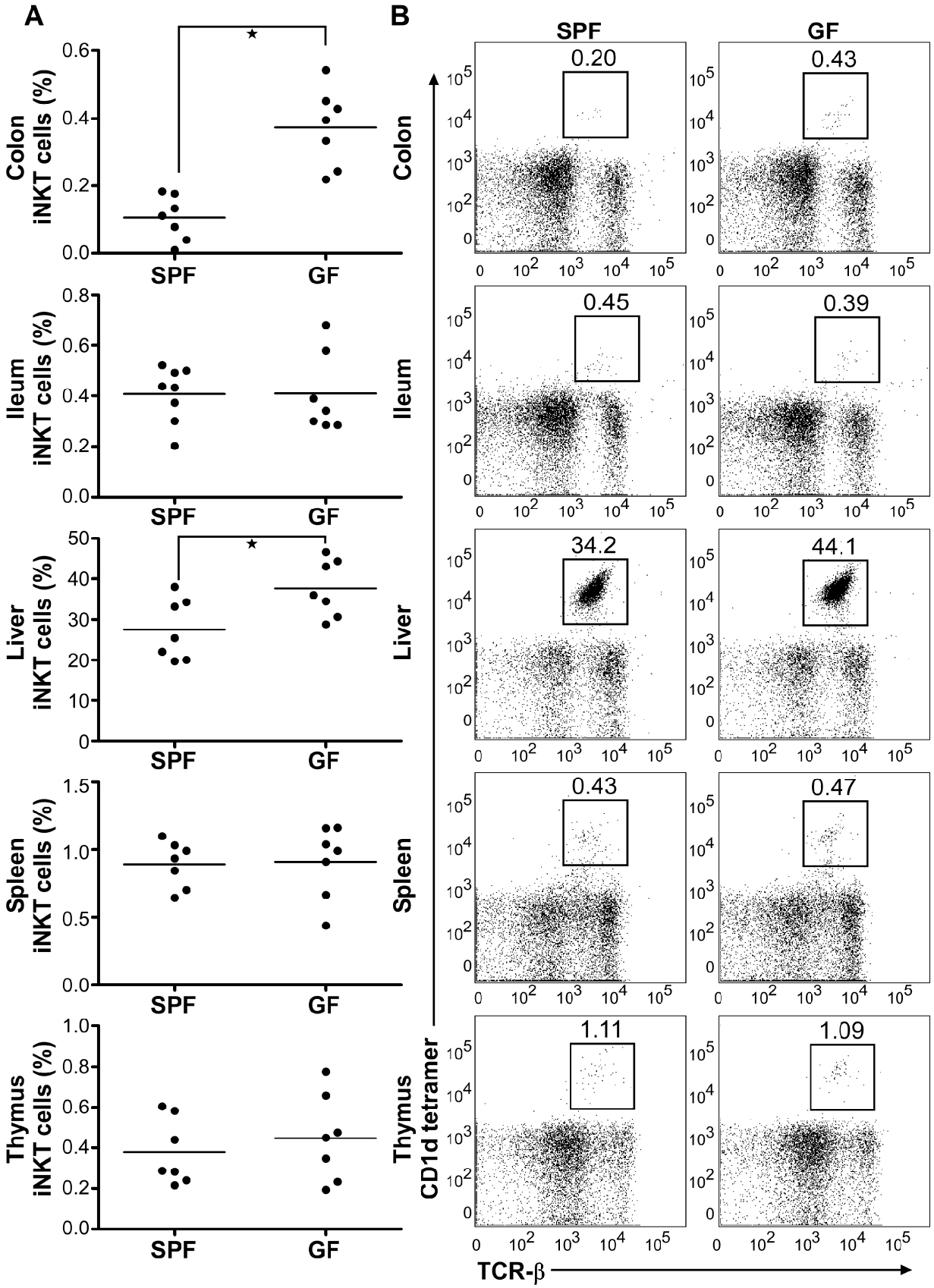


Fig. S2. Colonic and liver iNKT cells are increased in GF mice on a B6 genetic background. **(A)** Percentages for CD1d tetramer and TCR-β double positive cells (iNKT) of live lymphocytes from colon, ileum, liver, spleen and thymus of SPF and GF mice on a B6 background were analyzed by flow cytometry. Representative dot-plots are shown in **(B)**. All data were obtained from more than three independent experiments. Each circle represents a mouse, and error bars indicate SD. **P* ≤ 0.01, unpaired *t* test.

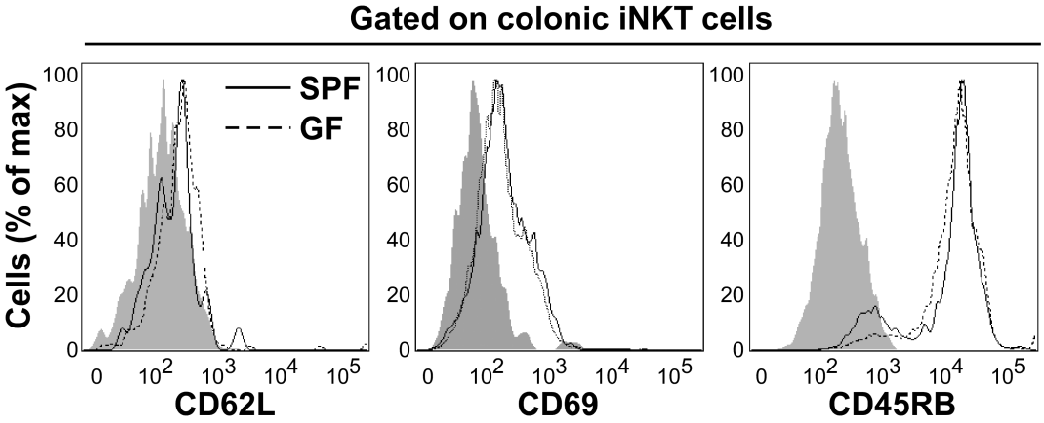


Fig. S3. Activation markers on iNKT cells in LP of SPF and GF mice show no differences. Colonic iNKT cells of live LP lymphocytes from SPF and GF mice were compared for the activation/proliferation markers CD62L, CD69 and CD45RB by flow cytometry. Representative histograms of three independent experiments are shown (n = 3 mice per group).

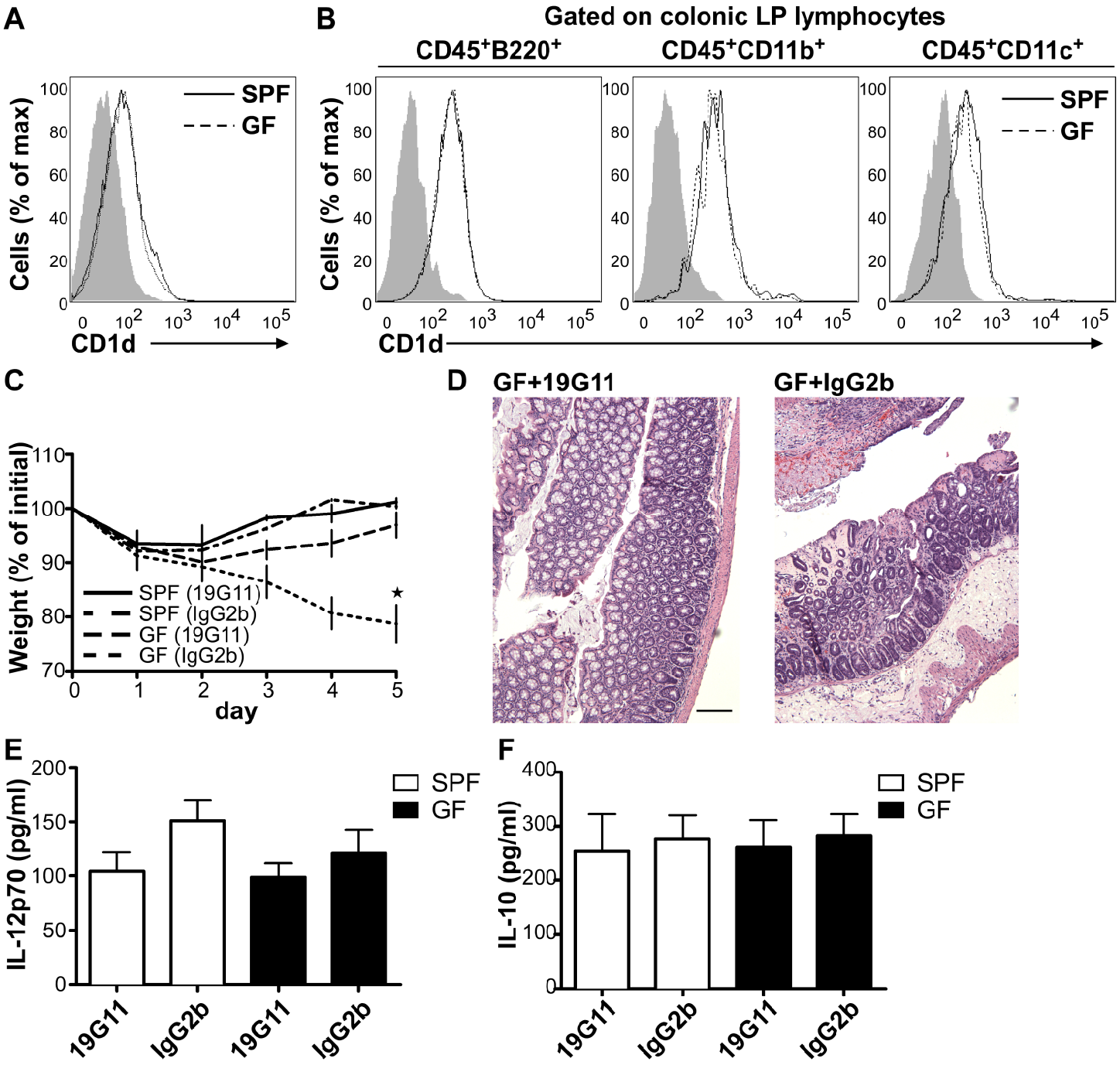


Fig. S4. CD1d-dependence of oxazolone-induced colitis in GF mice. **(A)** Colonic IECs of SPF and GF mice were isolated before rectal challenge with 1% oxazolone and analyzed for CD1d expression by flow cytometry (n ≥3 mice per group). **(B)** Colonic LP lymphocytes in gender matched SPF and GF mice were compared for surface CD1d expression within a CD45 and B220, CD11b or CD11c double positive population prior to rectal challenge. Representative histograms of three independent experiments are shown (n = 3 mice per group) **(C)** Age and gender matched SPF and GF mice were treated once before presensitization and rectal challenge with oxazolone with 1 mg 19G11 or IgG2b antibody and monitored for body weight loss for 5 days (n ≥ 4 mice per group). **(D)** On day five, the colons were collected and dissected for histological analysis by hematoxylin and eosin (H&E) staining. Representative images of the colon are shown from an i.p. 19G11 antibody-treated GF mouse and an IgG2b antibody-treated GF mouse (n = 3 mice per group). Bar represents 50 μm. **(E to F)** The concentration of IL-12p70 and IL-10 in the supernatants of 24 h-colon organ explant cultures determined by ELISA on day five after rectal challenge (n = 5 mice per group). All data were obtained from more than three independent experiments and error bars indicate SD. *$P \leq 0.05$, unpaired *t* test.

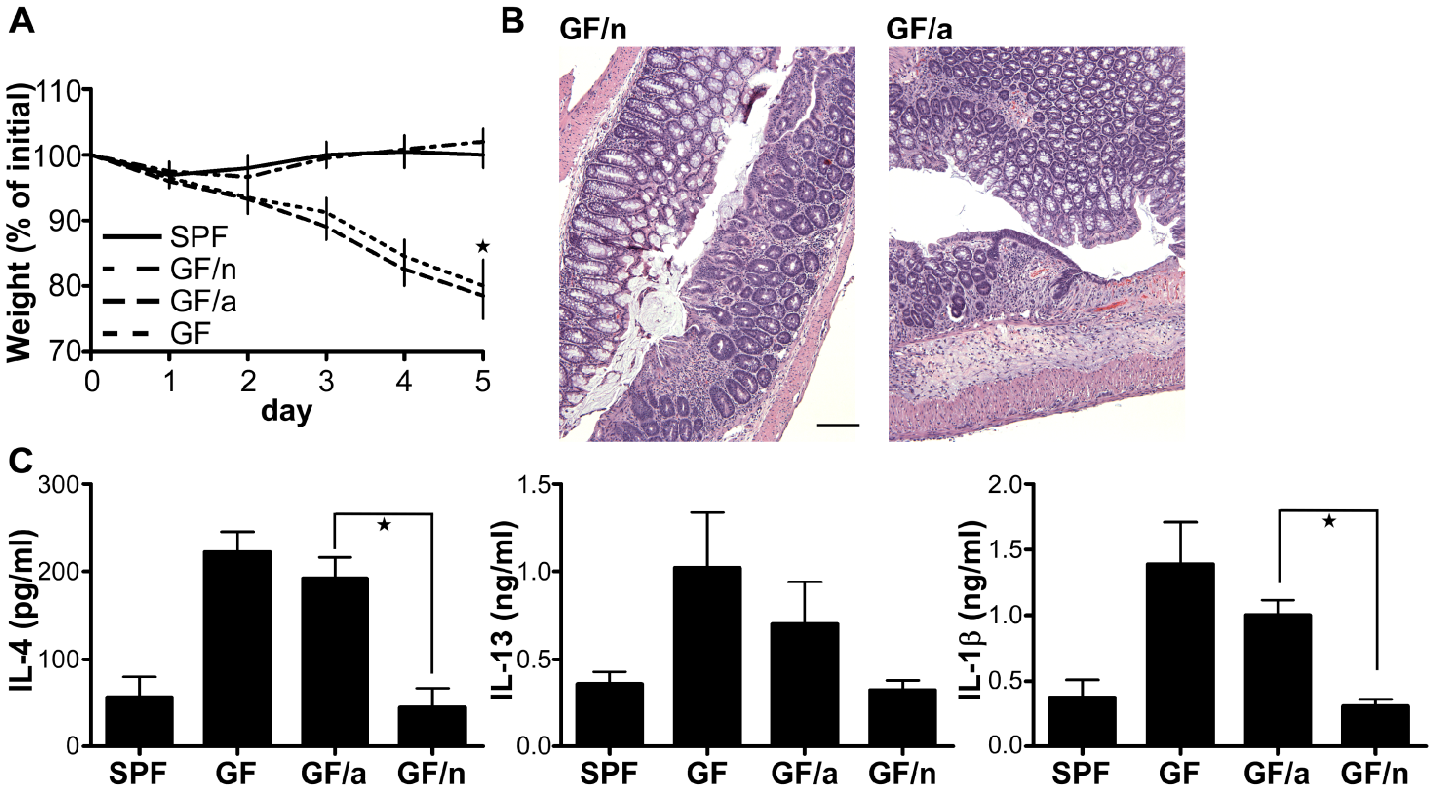


Fig. S5. Early exposure to conventional microorganisms protects from oxazolone colitis. **(A to C)** Induction of oxazolone colitis in 8-week-old GF mice either exposed continuously to conventional microbiota starting on their first day of life (GF/n) or at the age of five weeks (GF/a). The mice were monitored for body weight loss for five days (n = 5 mice per group). **(B)** Representative images of the colon are shown from a GF/n and GF/a mouse on day five after rectal challenge with oxazolone (n = 3 mice per group). Bar represents 50 μm. **(C)** The concentration of IL-4, IL-13 and IL-1 in the supernatant of 24 h colon explant cultures starting on day five after rectal challenge with oxazolone by ELISA (n = 4 mice per group). All data were obtained from more than two independent experiments with similar results and error bars indicate SD. *$P < 0.05$, unpaired *t* test.

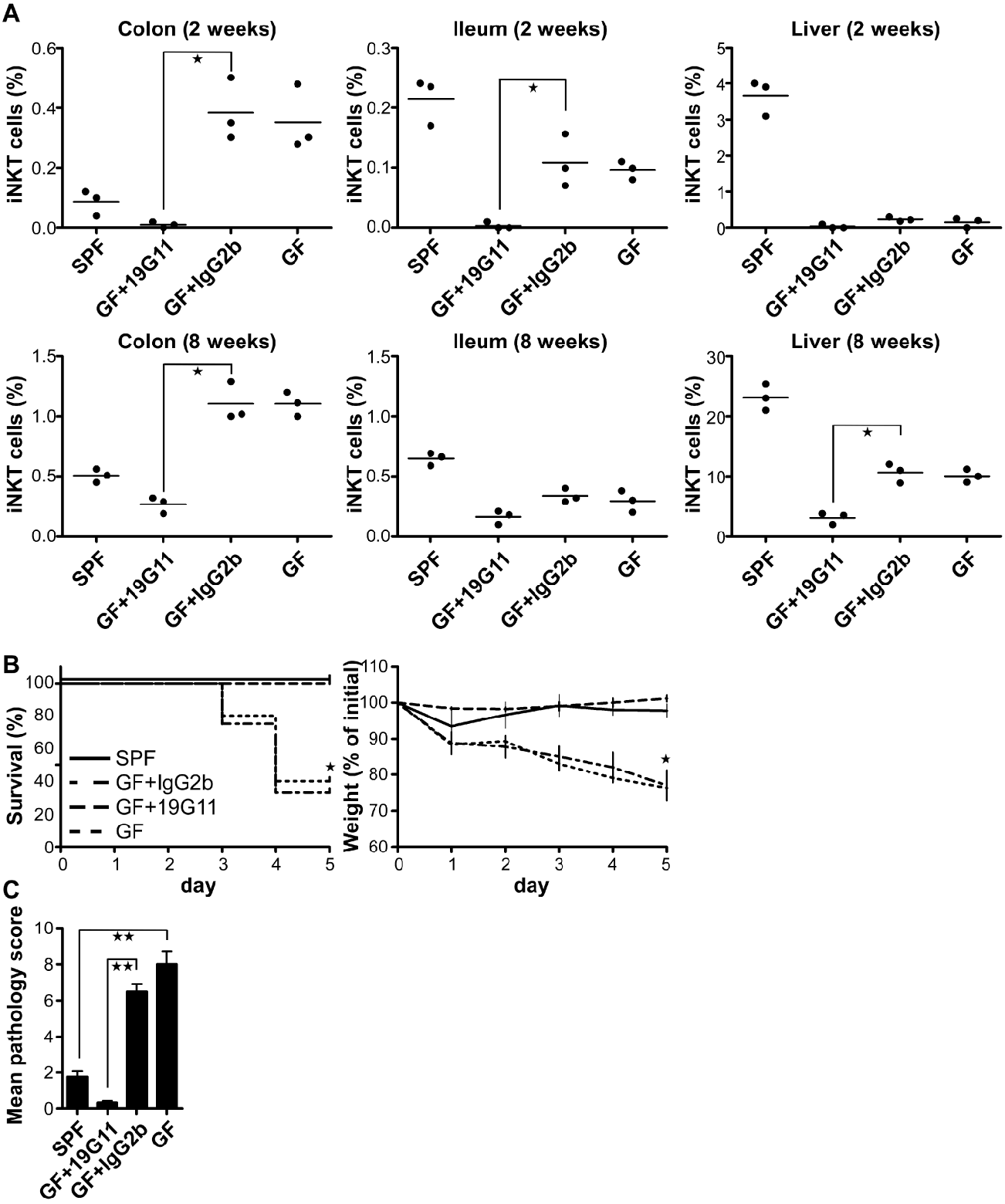


Fig. S6. Early-life effects of microbiota on iNKT cells is CD1d-dependent. **(A)** Percentages of iNKT cells of colonic and ileum LP lymphocytes and liver of SPF and GF mice at the age of two and eight weeks after treatment with 500 μg 19G11 or IgG2b antibody starting on day 1 of their lives and repeated 3 times a week for 2 weeks and continued afterwards once a week for 4 weeks. Each circle represents a mouse. **(B)** Eight-week old mice from each group were presensitized, rectally challenged with oxazolone and monitored and scored for survival (*P < 0.05, log-rank test) and body weight loss for five days (n = 5 mice per group). **(C)** On day five, the colons were collected and dissected for histological analysis (n ≥ 3 mice per group). All data were obtained from more than two independent experiments, and error bars indicate SD. *P < 0.05, **P ≤ 0.01, unpaired t test.

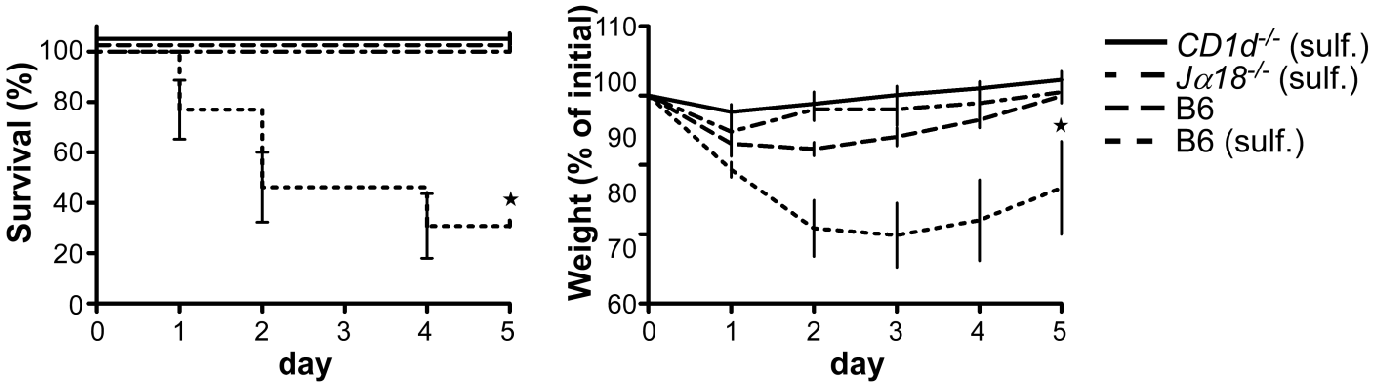


Fig. S7. Mice born under germ reduced conditions are more susceptible to oxazolone colitis. Pregnant females of *Cd1d*$^{-/-}$, *Jα18*$^{-/-}$ and B6 mice were treated with the antibiotic sulfatrim (sulf.) 24-48 hours before delivery and for two weeks thereafter. 4-week-old offspring mice were monitored and scored after rectal challenge with 1% oxazolone for survival (left panel) and body weight loss (right panel) for 5 days (n = 5 mice per group). All data were obtained from more than two independent experiments with similar results. Error bars represent the SD. **P* < 0.05, unpaired *t* test and **P* < 0.05, log-rank test.

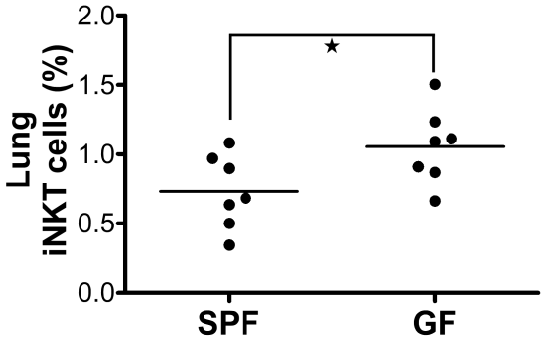


Fig. S8. Lung iNKT cells are increased in GF mice on a B6 genetic background. Percentages for CD1d tetramer and TCR-β double positive cells (iNKT) of live lymphocytes from lung of SPF and GF mice on a B6 background were analyzed by flow cytometry. All data were obtained from more than three independent experiments. Each circle represents a mouse. *$P \leq 0.05$, unpaired *t* test.

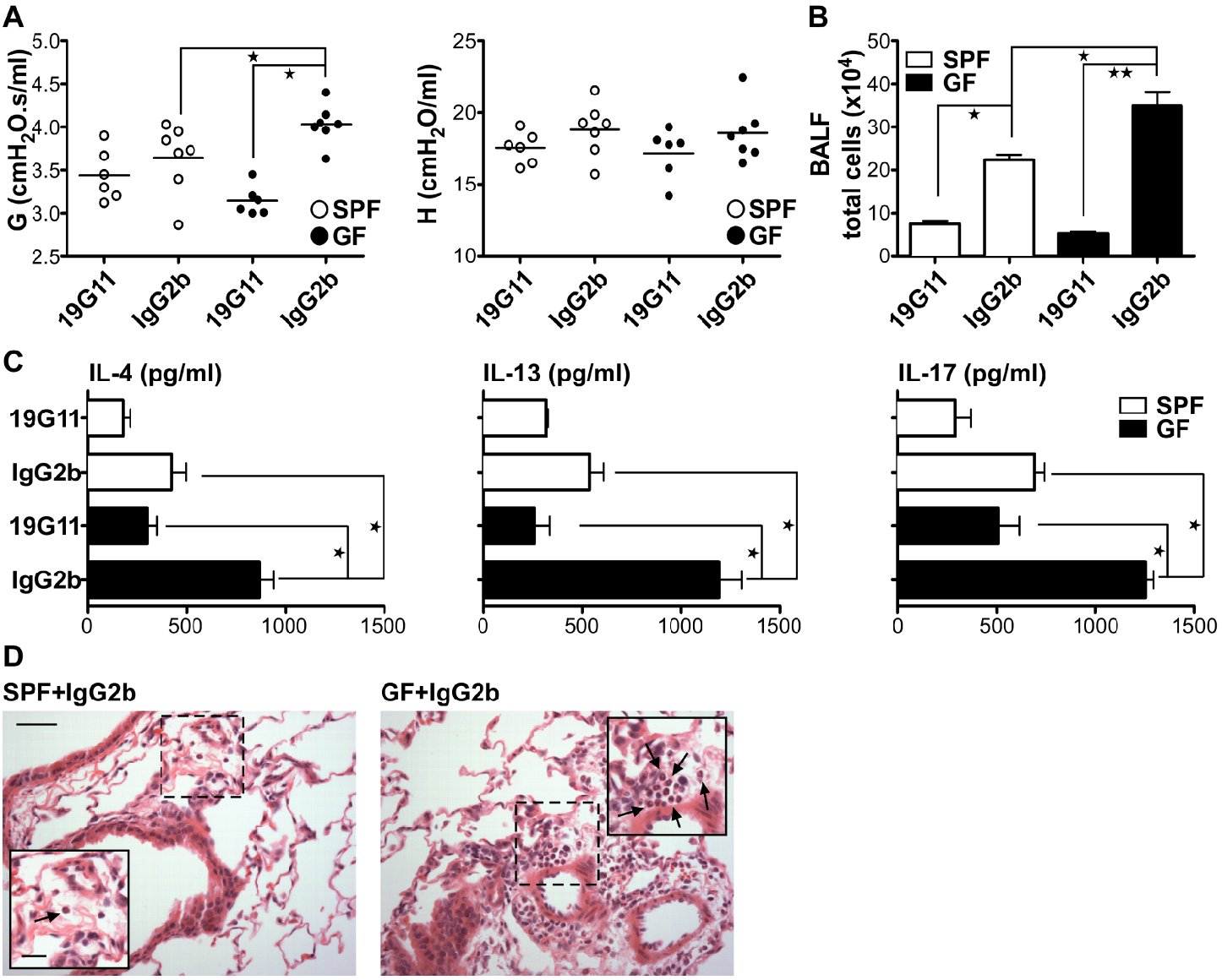


Fig. S9. GF mice are more susceptible to the development of allergic asthma. **(A)** SPF and GF mice were treated once i.p. with 1mg 19G11 or IgG2b antibody before presensitization with OVA and with 0.5 mg 19G11 or IgG2b antibody before the first and third serial OVA aerosolization. 24 h after the last serial 5% aerosolized OVA exposure the mice were analyzed with an invasive measurement for tissue resistance (G) and tissue elasticity (H). Each circle represents one mouse. **(B)** The BALF of each group was analyzed for the total cells (n = 6 mice per group). **(C)** IL-4, IL-13 and IL-17 concentration in the BALF (n = 4 mice per group). **(D)** Representative hematoxylin and eosin stains of SPF and GF mouse lungs is shown (arrows indicate eosinophils). Representative figures on n = 4 mice per group. Bar represents 50 μm. Data were obtained from more than two independent experiments with similar results. Error bars indicate SD. **P* < 0.05, ***P* < 0.01, unpaired *t* test.

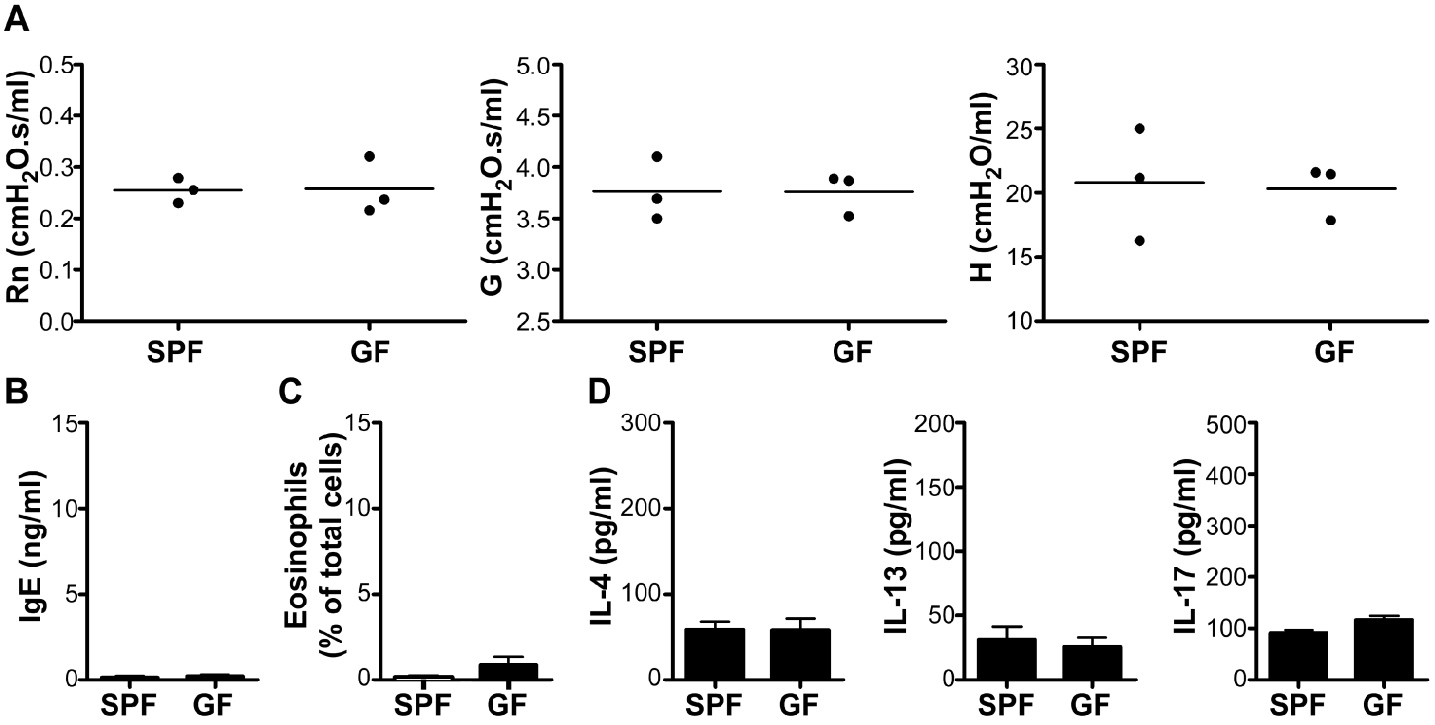


Fig. S10. GF mice do not exhibit pulmonary hyperresponsiveness at baseline. **(A)** Untreated 8-week-old SPF and GF mice were presensitized with OVA and analyzed for airway resistance (Rn), tissue resistance (G) and tissue elasticity (H) 24 h after the last serial aerosolization with PBS. Each circle represents a mouse. **(B)** Serum IgE level were measured by ELISA (n = 3 mice per group). **(C to D)** The BALF was analyzed for the percentage of eosinophils of the total BALF cells and the IL-4, IL-13 and IL-17 cytokine concentration of the BALF was measured by ELISA (n = 3 mice per group). All data were obtained from more than two independent experiments with similar results. Error bars indicate the SD.

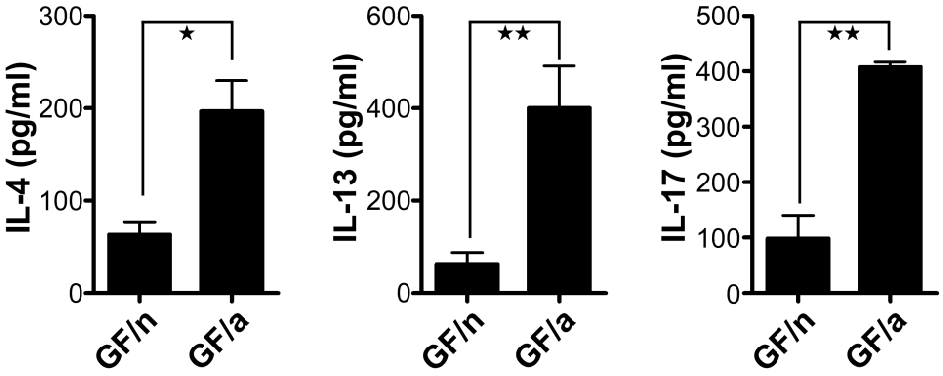


Fig. S11. Neonatal but not adult colonization protects from asthma. Age-matched mice from each group were presensitized with OVA and analyzed 24 h after the last challenge with 5% aerosolized OVA for IL-4, IL-13 and IL-17 concentration in the BALF (n ≥ 4 mice per group). All data were obtained from more than two independent experiments with similar results. Error bars indicate the SD. **P* ≤ 0.05, ***P* < 0.01, unpaired *t* test.

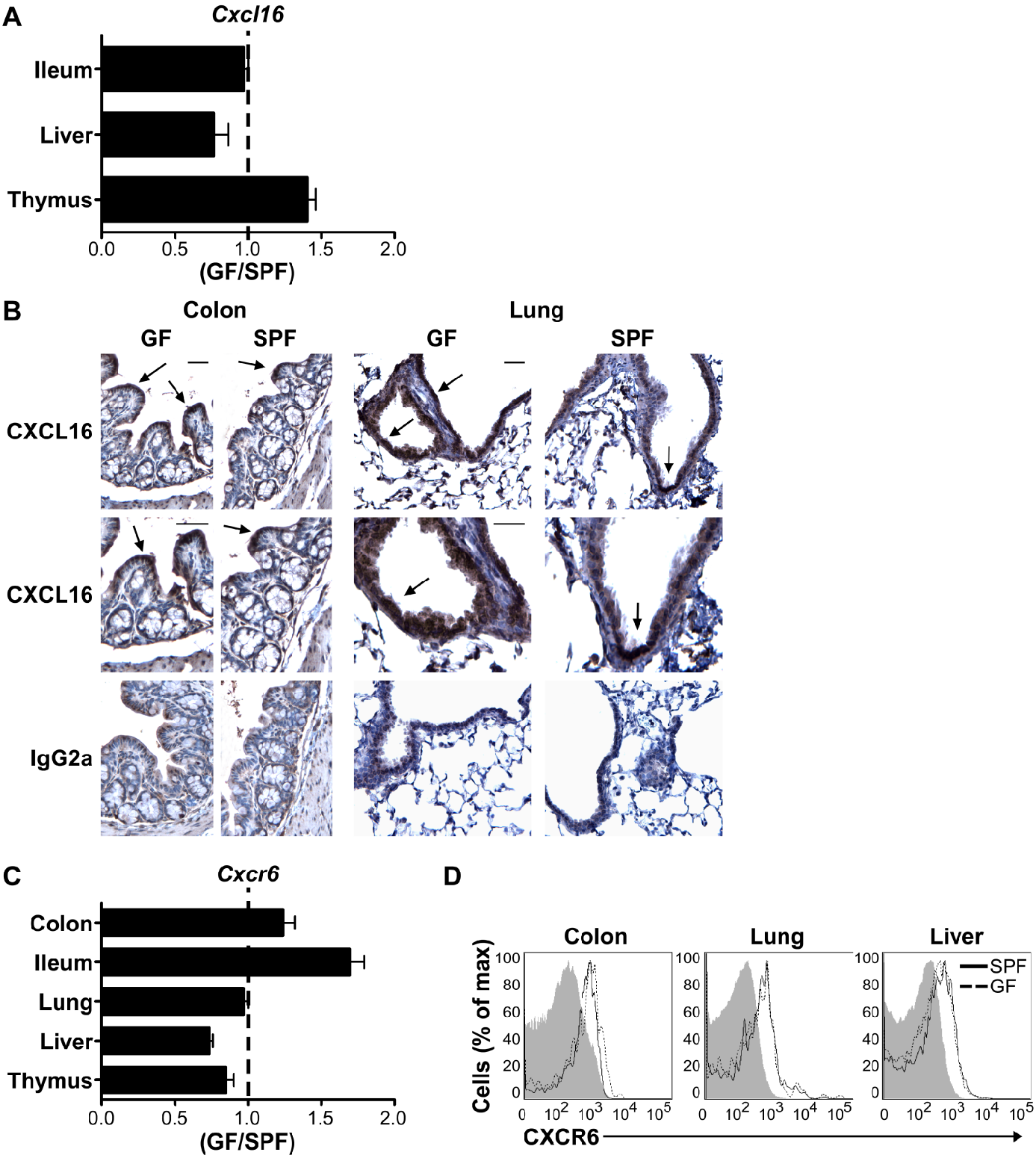


Fig. S12. Analysis of *Cxcl16* expression in tissues of SPF and GF mice. **(A)** Tissue samples from ileum, liver and thymus were collected from SPF and GF mice and the relative mRNA expression levels of the *Cxcl16* gene were analyzed (n = 5 mice per group). **(B)** Representative immunohistochemistry for CXCL16 staining and its isotype control IgG2a antibody in colon and lung of SPF and GF mice (n = 3 mice per group and arrows indicate positive staining). Bars represent 20 μm. **(C)** Tissue samples from colon, ileum, lung, liver and thymus were collected from SPF and GF mice and the relative mRNA expression levels of the *Cxcr6* gene were analyzed (n = 4 mice per group). **(D)** iNKT cells of live lymphocytes from colon, lung and liver of SPF and GF mice were analyzed for CXCR6 expression by flow cytometry (n = 3 mice per group). All data were obtained from three independent experiments with similar results. Error bars represent the SD. **P* ≤ 0.05, ***P* < 0.01, unpaired *t* test.

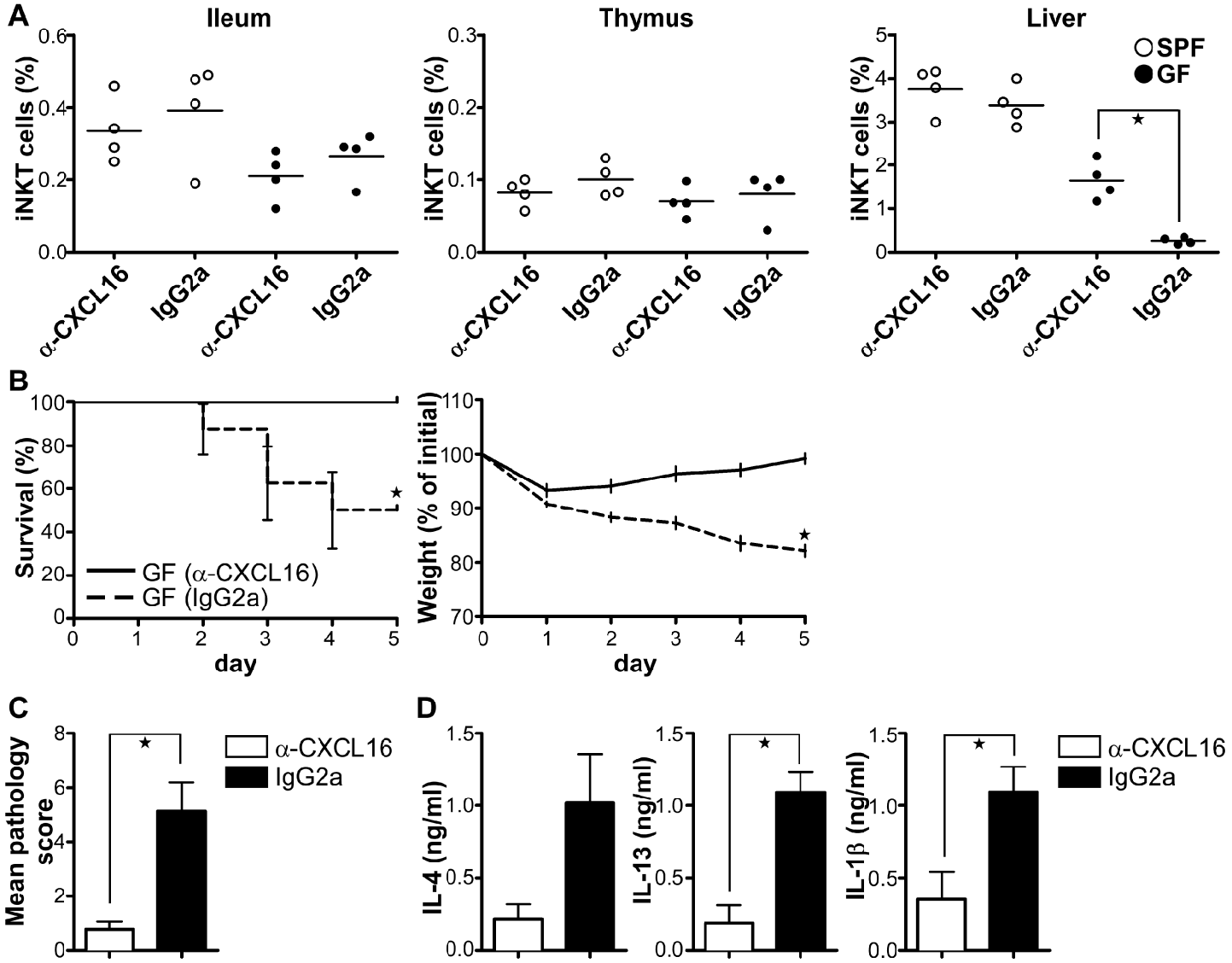


Fig. S13. iNKT cell homeostasis and role in colitis are CXCL16-dependent. **(A)** SPF and GF newborn mice were injected 3 times a week with 25 μg of a neutralizing CXCL16 antibody (α-CXCL16) or its isotype control IgG2a antibody and were analyzed at the age of 2 weeks for iNKT percentages by flow cytometry. Each circle represents a mouse. **(B)** 8-week-old GF littermates that were treated with 25 μg α-CXCL16 or IgG2a antibody 3 times a week for the first two weeks of life and afterwards once a week and were monitored and scored after rectal challenge with 1% oxazolone for survival and body weight loss for 5 days (n = 4 mice per group). **(C)** On day five, the colons were collected and dissected for histological analysis (n = 4 mice per group). **(D)** The concentration of IL-4, IL-13 and IL-1 in the supernatant of 24 h-colon organ explant cultures determined by ELISA on day five (n = 4 mice per group). All data were obtained from more than two independent experiments with similar results. Error bars represent the SD. **P* < 0.05, unpaired *t* test and **P* < 0.05, log-rank test.

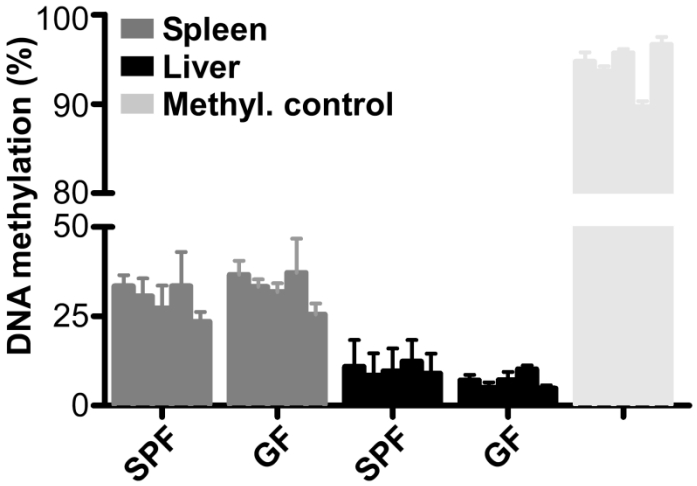


Fig. S14. Similar *Cxcl16* methylation in spleen and liver of SPF and GF mice. Analysis of DNA methylation of five CpG sites in the 5' region of *Cxcl16* by bisulfite pyrosequencing. For each group, the mean of DNA methylation of 5 CpG sites is shown as a percentage according to the methylated control (Methyl. control) (n ≥ 3 mice per group). All data were obtained from at least two independent experiments with similar results. Error bars represent the SD.

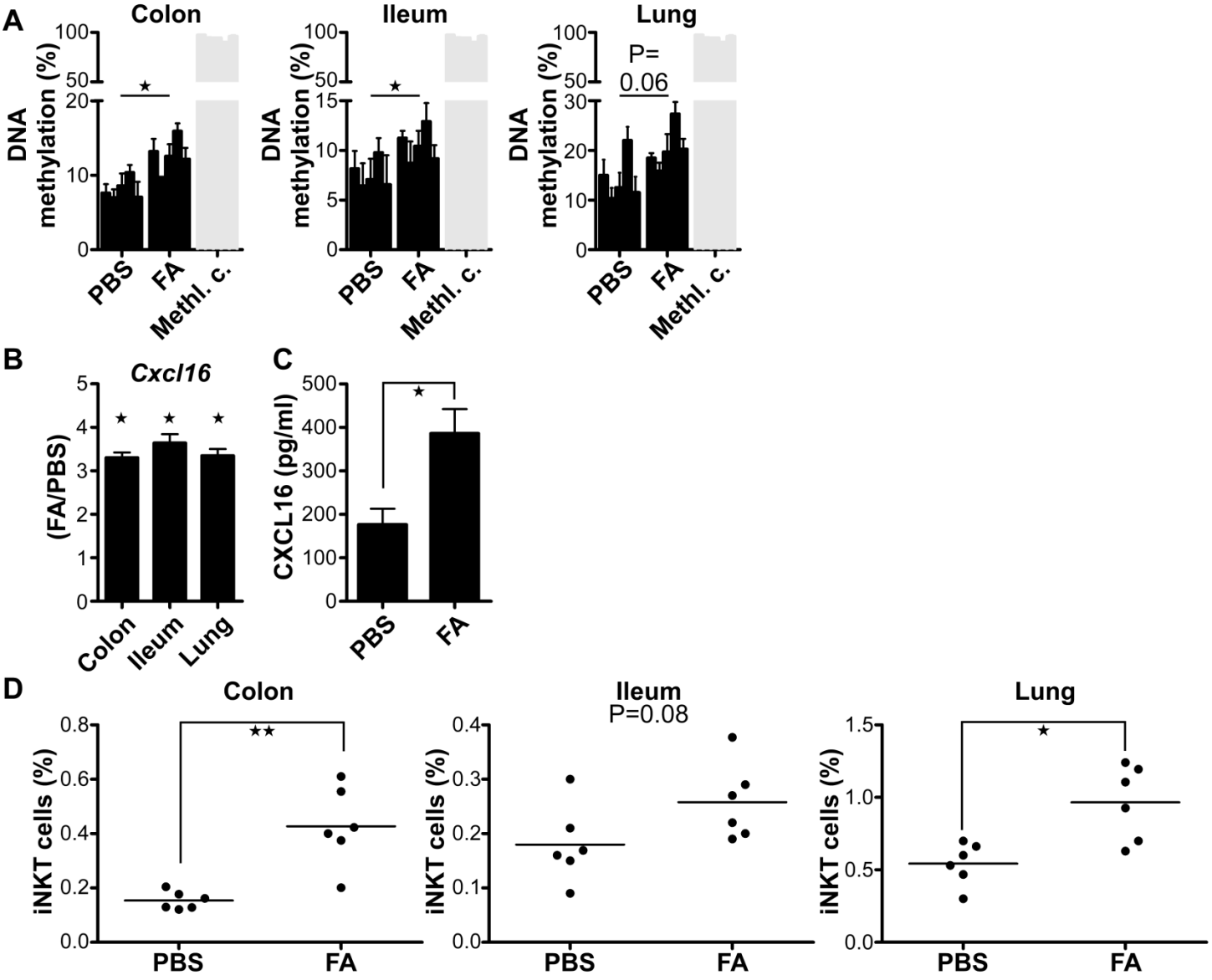


Fig. S15. Folinic acid treatment increases *Cxcl16* methylation and expression in SPF mice. SW SPF newborn littermates were orally gavaged 5 times a week for 2 weeks with 1 mg folinic acid (FA) or PBS. **(A)** Analysis of DNA methylation of five CpG sites in the 5' region of *Cxcl16* in different tissues by bisulfite pyrosequencing. For each group, the mean of DNA methylation of 5 CpG sites is shown as a percentage according to the methylated control (methyl. c.) (n ≥ 3 mice per group). **(B)** Tissue samples from colon, ileum and lung were collected from 2 week old FA and PBS treated SPF mice and the relative mRNA expression levels of the *Cxcl16* gene were analyzed by qPCR (n ≥ 3 mice per group). **(C)** The CXCL16 concentration in the serum of each group was measured by ELISA (n = 5 mice per group). **(D)** Percentages for iNKT cells of live lymphocytes from colon, ileum and lung of PBS or FA treated SPF mice were analyzed by flow cytometry. All data were obtained from more than two independent experiments. Each circle represents a mouse, and error bars indicate SD. *P ≤ 0.05, **P < 0.01, unpaired t test.

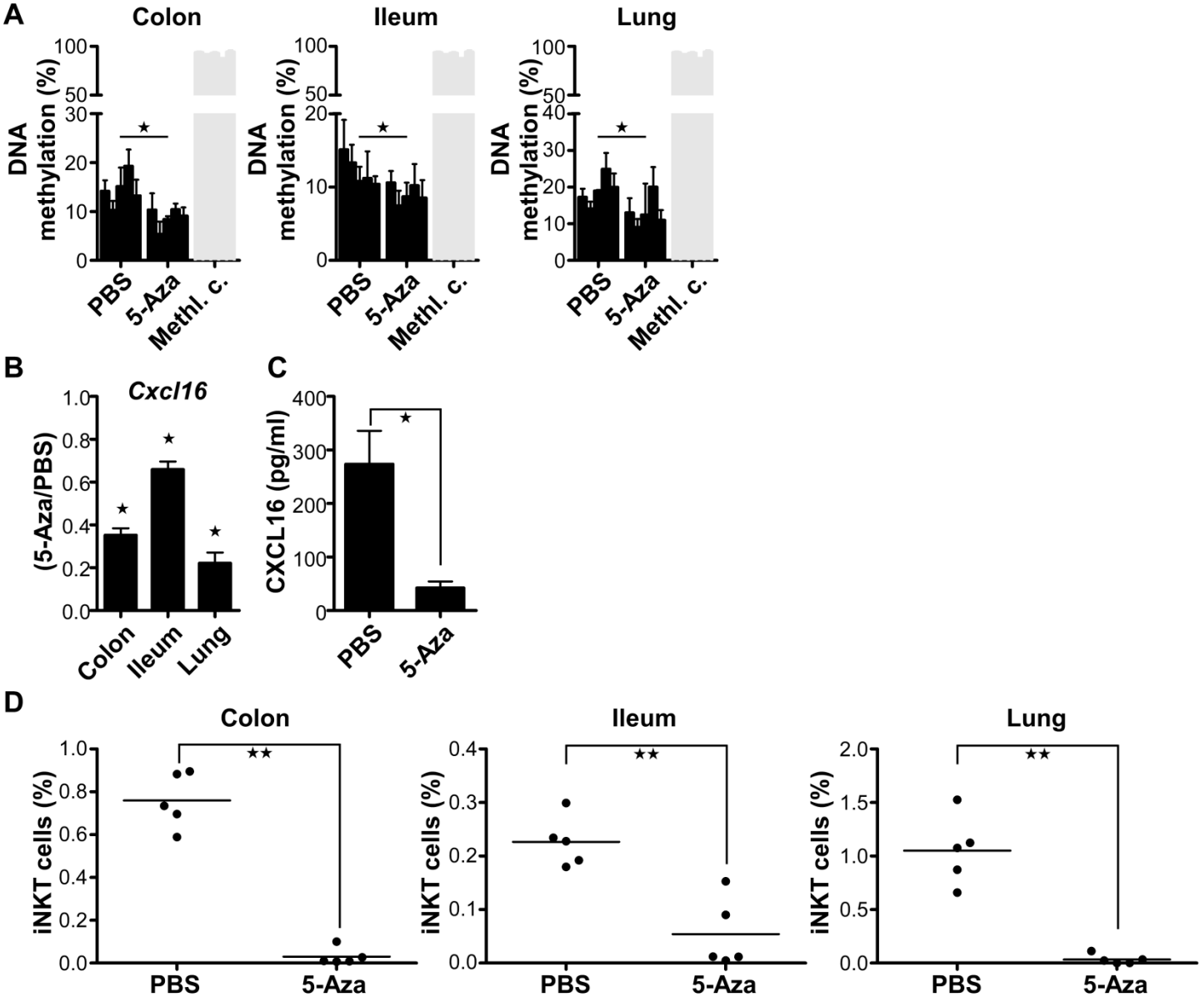


Fig. S16. 5-Azacytidine (5-Aza) treatment of GF mice decreases *Cxcl16* methylation and expression. SW GF newborn littermates were i.p. injected with 5-Aza or PBS on day 1 and day 8 of their lives. **(A)** Analysis of DNA methylation of five CpG sites in the 5' region of *Cxcl16* in different tissues by bisulfite pyrosequencing. For each group, the mean of DNA methylation of 5 CpG sites is shown as a percentage according to the methylated control (methyl. c.) (n ≥ 3 mice per group). **(B)** Tissue samples from colon, ileum and lung were collected from 5 weeks old 5-Aza and PBS treated GF mice and the relative mRNA expression levels of the *Cxcl16* gene were analyzed by qPCR (n ≥ 3 mice per group). **(C)** The CXCL16 concentration in the serum of each group was measured by ELISA (n = 5 mice per group). **(D)** Percentages for iNKT cells of live lymphocytes from colon, ileum and lung of PBS or 5-Aza treated GF mice were analyzed by flow cytometry. All data were obtained from more than two independent experiments. Each circle represents a mouse, and error bars indicate SD. *P ≤ 0.05, **P < 0.01, unpaired t test.

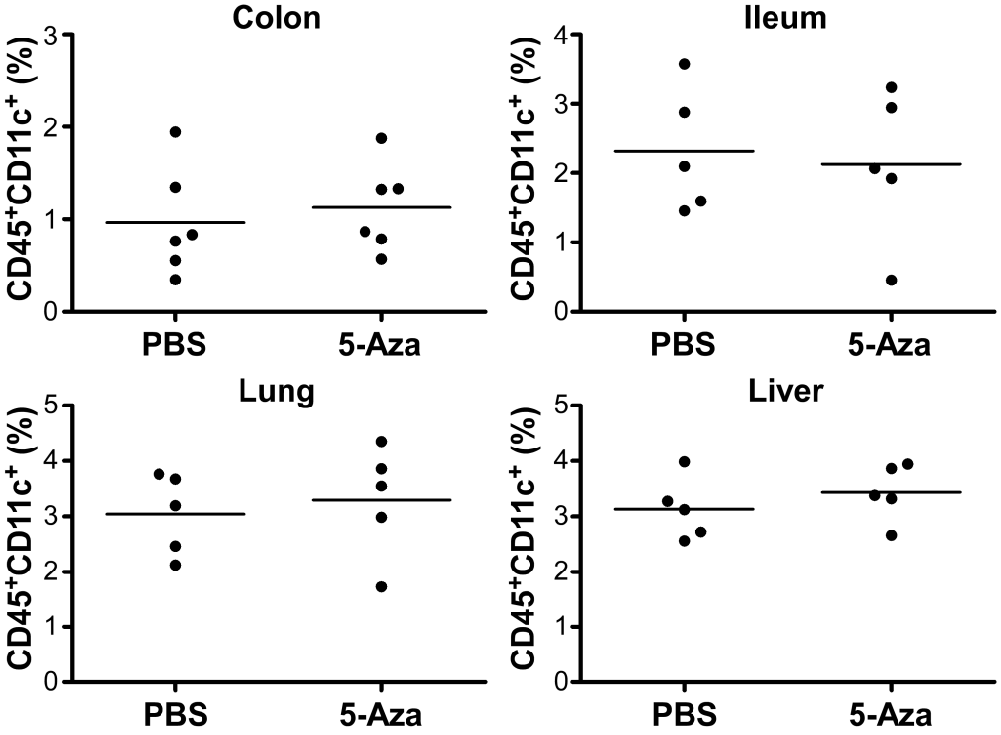


Fig. S17. Treatment with 5-Aza has no effects on dendritic cell numbers in tissues. SW GF newborn littermates were i.p. injected with 5-Aza or PBS on day 1 and day 8 of their lives. Percentages for $CD45^+CD11c^+$ double positive cells of live lymphocytes from colon, ileum, lung and liver of PBS or 5-Aza treated GF mice were analyzed by flow cytometry. All data were obtained from more than two independent experiments. Each circle represents a mouse, and error bars indicate SD.

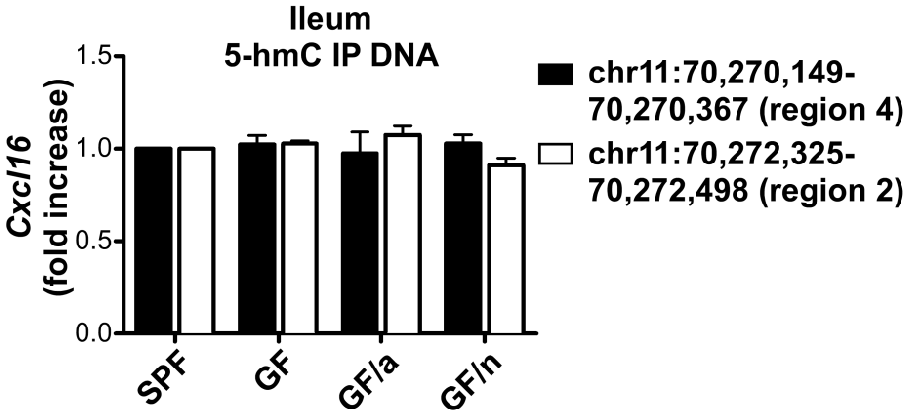


Fig. S18. 5-hydroxymethylation of *Cxcl16* in ileum is not affected by state of commensalism. *Cxcl16* qPCR analysis of ileal DNA after performing a 5-hydroxymethylated DNA immunoprecipitation (5-hmC IP DNA) ($n \geq 3$ mice per group). Data were obtained from two independent experiments with similar results. Error bars indicate the SD.

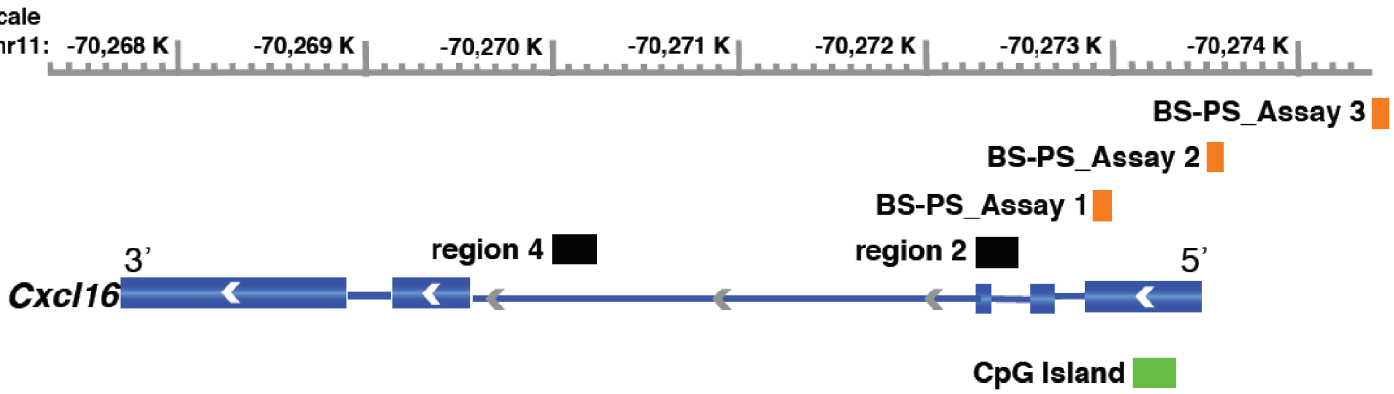


Fig. S19. Summary of *Cxcl16* gene analysis. Map with locations of regions optimized for bisulfite-pyrosequencing (BS-PS) used for *Cxcl16* analysis (UCSC genome browser version July 2007 (NCBI37/mm9), mouse (*Mus musculus*)). The *Cxcl16* gene contains a CpG island in its 5´end. BS-PS of three targetable regions within and around this CpG island could be optimized. However, only assay 2 exhibited differential DNA methylation at chr11:70,273,465-70,273,687 which contained five CpG sites as described in the text for the different groups. Two representative regions (region 2 and 4) are exhibited for *Cxcl16* analysis of 5-hmC modifications as defined by DNA immunoprecipitation and qPCR.

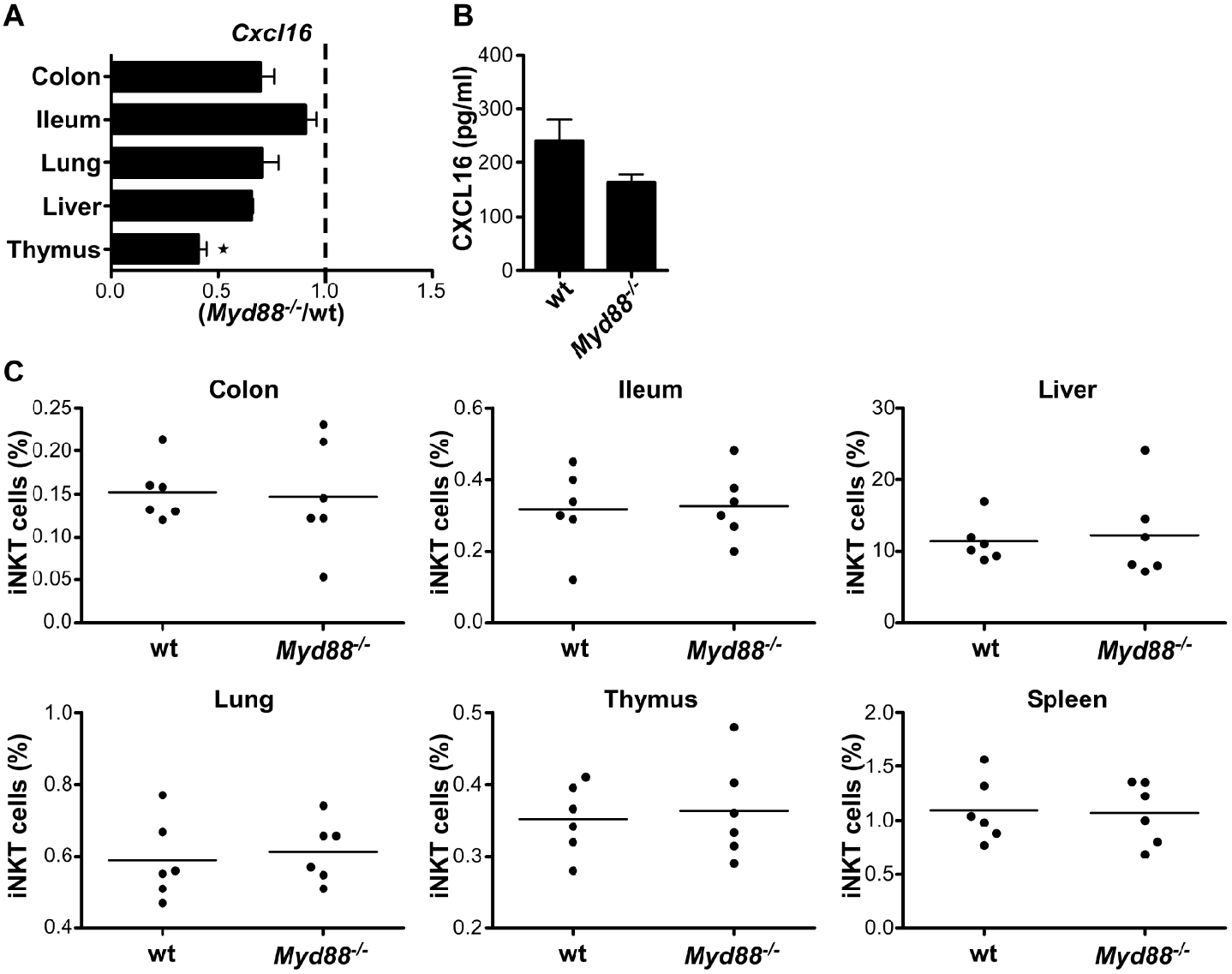


Fig. S20. Colonic and lung CXCL16 expression is *Myd88* independent. **(A)** *Cxcl16* mRNA expression levels in colon, ileum, lung, liver and thymus of B6 wildtype (wt) and *Myd88*$^{-/-}$ mice (n = 3 mice per group). **(B)** Serum CXCL16 expression in wt and *Myd88*$^{-/-}$ mice (n = 3 mice per group). Error bars indicate the SD. **(C)** Live lymphocytes from colon, ileum, lung, thymus, liver and spleen of 8-week-old wt and *Myd88*$^{-/-}$ mice were analyzed for iNKT cells by flow cytometry. All data were obtained from three independent experiments with similar results. Each circle represents a mouse. *$P < 0.05$, unpaired *t* test.

Table S1. Primers used for bisulfite pyrosequencing were:

Name	Sequence (5'-3')	5'-Modification	Annealing Temperature	Amplicon length	July 2010 (NCBI37/mm9)
CXCL_4FP	AGGTATTTTTTGGGTTTGGATTA	biotin	55°C	223 bp	chr11:70,273,465-70,273,687
CXCL_4RP	CTCAATAAAATCCAATCACATAAC				
CXCL_4seq	AAACCTATAAAAATACCC				

Table S2. Primers used for qPCR of gDNA were:

Name	Sequence (5'-3')	Annealing Temperature	Amplicon Length	July 2010 (NCBI37/mm9)
CXCL16 F1	TCTTCTGGCACCCAGATACC	60°C	216 bp	chr11:70,272,401-70,272,616
CXCL16 R1	AGAAGGTGAGCCCCACTACA			
CXCL16 F2	GGAACCTGCAAAAGGATCAA	60°C	174 bp	chr11:70,272,325-70,272,498
CXCL16 R2	GGACCATCGATCTGAACACC			
CXCL16 F3	GCAGGTGGATCTTGGTGAAT	60°C	205 bp	chr11:70,271,272-70,271,476
CXCL16 R3	CCACAAAACCCCAAAACAAC			
CXCL16 F4	TTCCTCATCCCTGTCTGTCC	60°C	219 bp	chr11:70,270,149-70,270,367
CXCL16 R4	GCTTTGCTGGGTCTCTCAAC			
CXCL16 F5	GTTGAGAGACCCAGCAAAGC	60°C	246 bp	chr11:70,269,923-70,270,168
CXCL16 R5	ACATTGAGATGTGGCATGGA			
CXCL16 F6	GGGAAGAGTTTTCACCACCA	60°C	167 bp	chr11:70,269,381-70,269,547
CXCL16 R6	GGTTGGGTGTGCTCTTTGTT			
CXCL16 F7	TCTCCCTTCAGGCTATGGTC	60°C	104 bp	chr11:70,269,262-70,269,365
CXCL16 R7	GTGTGCTAGCTCCAGCTCCT			
ACTB F	GATGCTCCCCGGGCTGTATT	60°C	225 bp	chr5:143,667,069-143,667,293
ACTB R	GGGGTACTTCAGGGTCAGGA			

References and Notes

1. D. Kelly, T. King, R. Aminov, Importance of microbial colonization of the gut in early life to the development of immunity. *Mutat. Res.* **622**, 58 (2007). doi:10.1016/j.mrfmmm.2007.03.011 Medline

2. H. Renz *et al*., *Nat. Rev. Immunol.* **12**, 9 (2012).

3. M. J. Ege *et al*.; GABRIELA Transregio 22 Study Group, Exposure to environmental microorganisms and childhood asthma. *N. Engl. J. Med.* **364**, 701 (2011). doi:10.1056/NEJMoa1007302 Medline

4. P. López-Serrano *et al*., Environmental risk factors in inflammatory bowel diseases. Investigating the hygiene hypothesis: A Spanish case-control study. *Scand. J. Gastroenterol.* **45**, 1464 (2010). doi:10.3109/00365521.2010.510575 Medline

5. E. von Mutius, Allergies, infections and the hygiene hypothesis—The epidemiological evidence. *Immunobiology* **212**, 433 (2007). doi:10.1016/j.imbio.2007.03.002 Medline

6. O. Akbari *et al*., Essential role of NKT cells producing IL-4 and IL-13 in the development of allergen-induced airway hyperreactivity. *Nat. Med.* **9**, 582 (2003). doi:10.1038/nm851 Medline

7. I. J. Fuss *et al*., Nonclassical CD1d-restricted NK T cells that produce IL-13 characterize an atypical Th2 response in ulcerative colitis. *J. Clin. Invest.* **113**, 1490 (2004). Medline

8. N. R. Cohen, S. Garg, M. B. Brenner, Antigen Presentation by CD1 Lipids, T Cells, and NKT Cells in Microbial Immunity. *Adv. Immunol.* **102**, 1 (2009). doi:10.1016/S0065-2776(09)01201-2 Medline

9. M. Kronenberg, Toward an understanding of NKT cell biology: Progress and paradoxes. *Annu. Rev. Immunol.* **26**, 877 (2005). doi:10.1146/annurev.immunol.23.021704.115742

10. B. Wei *et al*., Commensal microbiota and $CD8^+$ T cells shape the formation of invariant NKT cells. *J. Immunol.* **184**, 1218 (2010). doi:10.4049/jimmunol.0902620 Medline

11. F. Heller, I. J. Fuss, E. E. Nieuwenhuis, R. S. Blumberg, W. Strober, Oxazolone colitis, a Th2 colitis model resembling ulcerative colitis, is mediated by IL-13-producing NK-T cells. *Immunity* **17**, 629 (2002). doi:10.1016/S1074-7613(02)00453-3 Medline

12. G. Schiechl *et al*., Tumor development in murine ulcerative colitis depends on MyD88 signaling of colonic F4/80+CD11b(high)Gr1(low) macrophages. *J. Clin. Invest.* **121**, 1692 (2011). doi:10.1172/JCI42540 Medline

13. K. M. Maslowski *et al*., Regulation of inflammatory responses by gut microbiota and chemoattractant receptor GPR43. *Nature* **461**, 1282 (2009). doi:10.1038/nature08530 Medline

14. S. Rakoff-Nahoum, J. Paglino, F. Eslami-Varzaneh, S. Edberg, R. Medzhitov, Recognition of commensal microflora by toll-like receptors is required for intestinal homeostasis. *Cell* **118**, 229 (2004). doi:10.1016/j.cell.2004.07.002 Medline

15. W. Strober, I. J. Fuss, R. S. Blumberg, The immunology of mucosal models of inflammation. *Annu. Rev. Immunol.* **20**, 495 (2002). doi:10.1146/annurev.immunol.20.100301.064816 Medline

16. J. H. Roark *et al*., CD1.1 expression by mouse antigen-presenting cells and marginal zone B cells. *J. Immunol.* **160**, 3121 (1998). Medline

17. S. C. Yue, A. Shaulov, R. Wang, S. P. Balk, M. A. Exley, CD1d ligation on human monocytes directly signals rapid NF-κB activation and production of bioactive IL-12. *Proc. Natl. Acad. Sci. U.S.A.* **102**, 11811 (2005). doi:10.1073/pnas.0503366102 Medline

18. A. Mizoguchi, A. K. Bhan, A case for regulatory B cells. *J. Immunol.* **176**, 705 (2006). Medline

19. E. H. Meyer, R. H. DeKruyff, D. T. Umetsu, T cells and NKT cells in the pathogenesis of asthma. *Annu. Rev. Med.* **59**, 281 (2008). doi:10.1146/annurev.med.59.061506.154139 Medline

20. G. Wingender *et al*., Invariant NKT cells are required for airway inflammation induced by environmental antigens. *J. Exp. Med.* **208**, 1151 (2011). doi:10.1084/jem.20102229 Medline

21. C. Iwamura, T. Nakayama, Role of NKT cells in allergic asthma. *Curr. Opin. Immunol.* **22**, 807 (2010). doi:10.1016/j.coi.2010.10.008 Medline

22. T. Herbst *et al*., Dysregulation of allergic airway inflammation in the absence of microbial colonization. *Am. J. Respir. Crit. Care Med.* **184**, 198 (2011). doi:10.1164/rccm.201010-1574OC Medline

23. E. Germanov *et al*., Critical role for the chemokine receptor CXCR6 in homeostasis and activation of CD1d-restricted NKT cells. *J. Immunol.* **181**, 81 (2008). Medline

24. C. Day, R. Patel, C. Guillen, A. J. Wardlaw, The chemokine CXCL16 is highly and constitutively expressed by human bronchial epithelial cells. *Exp. Lung Res.* **35**, 272 (2009). doi:10.1080/01902140802635517 Medline

25. J. Diegelmann *et al*., Expression and regulation of the chemokine CXCL16 in Crohn's disease and models of intestinal inflammation. *Inflamm. Bowel Dis.* **16**, 1871 (2010). doi:10.1002/ibd.21306 Medline

26. V. Rishi *et al*., CpG methylation of half-CRE sequences creates C/EBPα binding sites that activate some tissue-specific genes. *Proc. Natl. Acad. Sci. U.S.A.* **107**, 20311 (2010). doi:10.1073/pnas.1008688107 Medline

27. M. Pufulete *et al*., Effect of folic acid supplementation on genomic DNA methylation in patients with colorectal adenoma. *Gut* **54**, 648 (2005). doi:10.1136/gut.2004.054718 Medline

28. C. X. Song *et al*., Selective chemical labeling reveals the genome-wide distribution of 5-hydroxymethylcytosine. *Nat. Biotechnol.* **29**, 68 (2011). doi:10.1038/nbt.1732 Medline

29. A. S. Neish, Microbes in gastrointestinal health and disease. *Gastroenterology* **136**, 65 (2009). doi:10.1053/j.gastro.2008.10.080 Medline

30. D. P. Strachan, Hay fever, hygiene, and household size. *BMJ* **299**, 1259 (1989). doi:10.1136/bmj.299.6710.1259 Medline

31. A. Hviid, H. Svanström, M. Frisch, Antibiotic use and inflammatory bowel diseases in childhood. *Gut* **60**, 49 (2011). doi:10.1136/gut.2010.219683 Medline

32. E. Goksör *et al*., Preschool wheeze—Impact of early fish introduction and neonatal antibiotics. *Acta Paediatr.* **100**, 1561 (2011). doi:10.1111/j.1651-2227.2011.02411.x Medline

33. B. A. Sullivan, M. Kronenberg, TCR-mediated recognition of glycolipid CD1 complexes. *Curr. Top. Microbiol. Immunol.* **314**, 165 (2007). doi:10.1007/978-3-540-69511-0_7 Medline

34. K. A. Sauer, P. Scholtes, R. Karwot, S. Finotto, Isolation of $CD4^+$ T cells from murine lungs: A method to analyze ongoing immune responses in the lung. *Nat. Protoc.* **1**, 2870 (2006). doi:10.1038/nprot.2006.435 Medline

35. J. L. Matsuda *et al*., Tracking the response of natural killer T cells to a glycolipid antigen using CD1d tetramers. *J. Exp. Med.* **192**, 741 (2000). doi:10.1084/jem.192.5.741 Medline

36. R. M. Baron *et al*., Nitric oxide synthase-2 down-regulates surfactant protein-B expression and enhances endotoxin-induced lung injury in mice. *FASEB J.* **18**, 1276 (2004). Medline

37. B. Lamprecht *et al*., Derepression of an endogenous long terminal repeat activates the CSF1R proto-oncogene in human lymphoma. *Nat. Med.* **16**, 571, 1p, 579 (2010). doi:10.1038/nm.2129 Medline